Endocrine Reviews, 2022, Vol. 43, No. 1, 61–90
doi:10.1210/endrev/bnab017
Review

Review

Osteogenesis Imperfecta: Mechanisms and Signaling Pathways Connecting Classical and Rare OI Types

Milena Jovanovic,[1,*] Gali Guterman - Ram,[1,*] and Joan C. Marini[1]

[1]Section on Heritable Disorders of Bone and Extracellular Matrix, Eunice Kennedy Shriver National Institute of Child Health and Human Development, National Institutes of Health, Bethesda, MD, USA

*These authors contributed equally.

ORCiD numbers: 0000-0001-8797-0031 (M. Jovanovic); 0000-0002-8583-3401 (G. Guterman-Ram); 0000-0002-3685-0950 (J. C. Marini).

Abbreviations: ATF6, activating transcription factor 6; BBF2H7, 3′,5′-cyclic adenosine 5′-monophosphate responsive element binding protein 3-like 2 transcription factor; BFR, bone formation rate; BiP, heat shock protein family A (Hsp70) member 5; BMDD, bone mineral density distribution; BMP, bone morphogenetic protein; BMP1, bone morphogenetic protein 1; BP, bisphosphonates; BRIL, bone-restricted interferon-induced transmembrane protein-like protein;BV, bone volume; BV/TV, bone volume over total volume; Ca, calcium; COPII, coat complex component; DXA, dual-energy X-ray absorptiometry, bone densitometry; ECM, extracellular matrix; ER, endoplasmic reticulum; ERK, extracellular signal-regulated kinase; FKBP11, FKBP prolyl isomerase 11; Hsp47, heat shock protein 47; IFITM5, interferon-induced transmembrane protein 5; IP3R, inositol 1,4,5-trisphosphate receptor; KDELR2, KDEL endoplasmic reticulum protein retention receptor 2;LH1, lysyl hydroxylase 1; LRP5, low-density lipoprotein receptor-related protein 5; LRP6, low-density lipoprotein receptor-related protein 6; MAPK, mitogen-activated protein kinase; MAR, mineral apposition rate; MESD, low-density lipoprotein receptor-related protein chaperone MESD; NCP, noncollagenous proteins; OASIS, old astrocyte specifically induced-substance; OI, osteogenesis imperfecta; P3H1, prolyl 3-hydroxylase 1; PDI, protein disulfide isomerase; PEDF, pigment epithelium-derived factor;PERK, eukaryotic translation initiation factor 2 alpha kinase 3; PTC, premature termination codons; qBEI, quantitative backscattered electron imaging; QOL, quality of life; RIP, regulated intramembrane proteolysis; S1P, site-1 protease; S2P, site-2 protease; SERPINF1, serpin family F member 1; SR, sarcoplasmic reticulum; TbN, trabecular number; TGFβ, transforming growth factor-beta; TMEM38B, transmembrane protein 38B; TRIC, trimeric intracellular cation;UPR, unfolded protein response; WNT1, Wnt family member 1; WT, wild-type.

First Published Online: 18 May 2021; Corrected and Typeset: 31 July 2021.

Abstract

Osteogenesis imperfecta (OI) is a phenotypically and genetically heterogeneous skeletal dysplasia characterized by bone fragility, growth deficiency, and skeletal deformity. Previously known to be caused by defects in type I collagen, the major protein of extracellular matrix, it is now also understood to be a collagen-related disorder caused by defects in collagen folding, posttranslational modification and processing, bone mineralization, and osteoblast differentiation, with inheritance of OI types spanning autosomal dominant and recessive as well as X-linked recessive. This review provides the latest updates on OI, encompassing both classical OI and rare forms, their mechanism, and

ISSN Print: 0163-769X
ISSN Online: 1945-7189
Printed: in USA

the signaling pathways involved in their pathophysiology. There is a special emphasis on mutations in type I procollagen C-propeptide structure and processing, the later causing OI with strikingly high bone mass. Types V and VI OI, while notably different, are shown to be interrelated by the interferon-induced transmembrane protein 5 p.S40L mutation that reveals the connection between the bone-restricted interferon-induced transmembrane protein-like protein and pigment epithelium-derived factor pathways. The function of regulated intramembrane proteolysis has been extended beyond cholesterol metabolism to bone formation by defects in regulated membrane proteolysis components site-2 protease and old astrocyte specifically induced-substance. Several recently proposed candidate genes for new types of OI are also presented. Discoveries of new OI genes add complexity to already-challenging OI management; current and potential approaches are summarized.

Key Words: osteogenesis imperfecta, collagen synthesis, bone mass, bone mineralization, PEDF, regulated intramembrane proteolysis, *IFITM5*/BRIL, *MBTPS2*

Graphical Abstract

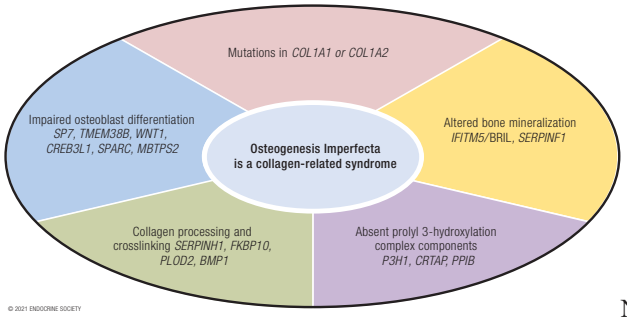

NICHD IRP

ESSENTIAL POINTS

- Osteogenesis imperfecta (OI) or "brittle bone" disease is a hereditary skeletal dysplasia associated with bone fragility, growth deficiency, and variable secondary features.
- OI is now understood to be a collagen-related disorder, caused by defects not only in collagen structure but also in genes that affect collagen folding, posttranslational modification and processing, bone mineralization, and osteoblast differentiation.
- Defects directly in type I collagen structure or quantity cause 80% to 85% of cases.
- Defects in processing or structure of type I procollagen propeptides cause distinctive OI forms, including paradoxical high bone mass OI from defects in C-propeptide processing.
- The cellular pathways of types V [*IFITM5*/bone-restricted interferon-induced transmembrane protein-like protein (BRIL) 5' MALEP] and VI (*PEDF*) OI are revealed to connect by BRIL p.S40L substitution with symptoms, histology, and molecular findings of pigment epithelium-derived factor deficiency.
- OI caused by defects in components (site-2 protease, old astrocyte specifically induced-substance) of regulated membrane proteolysis (RIP) expand the function of RIP beyond cholesterol metabolism to bone development.
- Current pharmacological therapy includes antiresorptive bisphosphonates, with variable results; anabolic antisclerostin antibody shows promise in animal models for increasing bone strength without increasing bone brittleness.

Table 1. Osteogenesis Imperfecta genetic classification and unique features

OI type	Inheritance	Defective gene	Protein	OMIM	Locus	Hypermineralization	Distinguishing features
Defects in collagen structure and processing							
I	AD	COL1A1	Collagen α1	166 200	17q21.33	YES	Loss of function of one of COL1A1 alleles
II-IV	AD	COL1A1, COL1A2	Collagen α1 or α2	166 210, 259 420, 166 220	17q21.33, 7q21.3	YES	Structural defects in collagen helix or C-propeptides
Procollagen Processing							
OI/EDS	AD	COL1A1, COL1A2	Procollagen α1 or α2	N/A	17q21.33, 7q21.3	YES	Defects in 90 residues at N-terminus of collagen helix that decrease pN-processing
HBM	AD	COL1A1, COL1A2	Collagen α1 or α2	N/A	17q21.33	YES	Defects in C-propeptide cleavage site, DXA normal to increased
XIII	AR	BMP1	BMP1	614 856	8p21.3	YES	Deficiency of C-propeptidase
Bone mineralization defects							
V	AD	IFITM5	BRIL (BRIL5' MALEP)	610 967	11p15.5	YES	Calcification of interosseous membrane, dense metaphyseal band, hyperplastic callus, mesh- like pattern in lamellar bone
Atypical VI	AD	IFITM5	BRIL (BRIL Ser40Leu)	610 967	11p15.5	YES	Increased osteoid, fish-scale pattern in lamellar bone, increased ALP levels in childhood, sx onset at birth
VI	AR	SERPINF1	PEDF	613 982	17p13.3	YES	PEDF deficiency, increased osteoid, fish-scale pattern in lamellar bone, increased ALP levels in childhood, onset after age 1 year
Defects in collagen modification							
VII	AR	CRTAP	CRTAP	610 682	3q22.3	YES	Absent procollagen prolyl 3-hydroxylation; full over modification, rhizomelia, white sclerae
VIII	AR	LERPE1	P3H1	610 915	1p34.2	YES	Absent procollagen prolyl 3-hydroxylation; full over modification, rhizomelia, "popcorn" metaphyses; white sclerae
IX	AR	Peptidylprolyl isomerase B	CyPB	259 440	15q22.31	YES	Absent procollagen prolyl 3-hydroxylation; helix mod varies, no rhizomelia, white sclerae
XIV	AR	TMEM38B	TRIC-B	615 066	9q31.2	NO	Decreased modification of collagen helix
Defects in collagen folding and cross-linking							
X	AR	SERPINH1	HSP47	613 848	11q13.5	ND	Severe skeletal deformity, blue sclerae, dentinogenesis imperfecta, skin abnormalities, inguinal hernias

Table 1. Continued

OI type	Inheritance	Defective gene	Protein	OMIM	Locus	Hypermineralization	Distinguishing features
NA	AR	KDELR2	KDEL endoplasmic reticulum protein retention receptor	619 131	7p22.1	ND	Short stature, progressive skeletal deformation, white sclerae, chest wall deformities
XI	AR	FKBP10	FKBP65	610 968	17q21.2	YES	May have congenital contractures
NA	AR	PLOD2	LH2	609 220	3q24	YES	Progressive joint contractures
Osteoblast function and differentiation							
XII	AR	SP7	OSTERIX	613 849	12q13.13	ND	Severe skeletal deformity, delayed tooth eruption, facial hypoplasia
XV	AD/AR	WNT1	WNT1	615 220	12q13.12	NO	May have neurological defects
XVI	AR	CREB3L1	OASIS	616 215	11p11.2	YES	Defect in RIP pathway
XVII	AR	SPARC	SPARC	616 507	5q33.1	YES	Progressive severe bone fragility
XVIII	XR	MBTPS2	S2P	301 014	Xp22.12	YES	X-linked OI, defect in RIP pathway, rhizomelia
Unclassified disorders							
NA	AR	FAM46A	FAM46A	617 952	6q14.1	ND	Defect in BMP/TGFβ signaling pathway
NA	AR	MESD	LRP chaperone MESD	618 644	15q25.1	ND	Could also be classified with LRP5/6 related disorders
NA	AR	Coiled-coil domain-containing protein 134	Coiled-coil domain-containing protein 134	618 788	22q13.2	ND	Could also be classified with MAPK/ERK skeletal dysplasias

Abbreviations: AD, autosomal dominant; AR, autosomal recessive; COL1A1, collagen type I alpha 1 chain; COL1A2, collagen type I alpha 2 chain; CREB3L1, 3′,5′-cyclic adenosine 5′-monophosphate responsive element binding protein 3-like 1; CRTAP, cartilage-associated protein; CyPB, cyclophilin B; FAM46A, terminal nucleotidyltransferase 5A; FKBP10, FKBP prolyl isomerase 10; FKBP65, FKBP prolyl isomerase 65; KDELR2, KDEL endoplasmic reticulum protein retention receptor 2; LH2, lysyl hydroxylase 2; MBTPS2, membrane-bound transcription factor peptidase site 2; SERPINH1, serpin family H member 1; SPARC, secreted protein acidic and cysteine rich; XR, X-linked recessive.

Osteogenesis imperfecta (OI) or "brittle bone disease" is a rare hereditable skeletal dysplasia with an incidence of 1 in 15 000 to 20 000 live births. It is characterized clinically by bone fragility, skeletal deformities, and short stature. In addition to its bone phenotype, OI affects the function of other connective tissues, causing various combinations of dentinogenesis imperfecta, hearing loss, joint hypermobility, blue sclerae, basilar invagination, and cardio/respiratory defects. The classical OI types I to IV, described in the Sillence classification, are dominantly inherited disorders caused by structural or quantitative defects in the *COL1A1* or *COL1A2* genes that encode the α1(I) and α2(I) chains of collagen type I, respectively. The clinical outcome ranges from mild to moderate to severe phenotypes for OI types I, IV, and III, respectively, as well as to a perinatal lethal outcome in OI type II.

The unifying feature of OI as a collagen-related disorder of connective tissue begins to guide us in diagnosing OI in an individual or in assigning defects in a particular gene as "OI-causing." The defining features of OI have emerged as our understanding of OI genetics has grown. The field may well be overdue for a consensus conference of the sort conducted periodically for Ehlers-Danlos syndrome, stipulating major and minor features for diagnosis. At the present, a combination of features in type I collagen, clinical manifestations, bone tissue, and cellular abnormalities influence our appraisal of which sets of gene defects constitute OI.

First, defects in the structure or quantity of type I collagen is key—including decreased transcripts, decreased secretion due to ER retention, altered posttranslational modification, propeptide processing or cross-linking, and abnormal fibrils in tissue. Each type will have some but not all of these collagen abnormalities. Second, clinically, we find bone fragility, manifest as fractures and vertebral compressions, as well as bowing deformity, although not all affected individuals fracture and many fragility disorders are not OI. Short stature of some degree is generally part of OI. Many individuals have secondary skeletal features such as dentinogenesis imperfecta, conductive hearing loss, mild facial dysmorphism, or relative macrocephaly. As a generalized connective tissue disorder, abnormal function of the respiratory and cardiac systems is not rare. Third, bone tissue is characterized by low bone mass, with a thin cortex and decreased bone volume/tissue volume (BV/TV) due to decreased trabecular number (TbN) and mineral apposition rate (MAR)/bone formation rate (BFR). Whole bone is less stiff and fractures at a lower load, with a key OI feature of brittleness or decreased displacement before fracturing. Another key feature of OI bone, hypermineralization, underlies its brittleness. The almost uniformly low dual-energy X-ray absorptiometry (DXA) bone density of OI reflects a phantom-based measurement, while direct measurements of bone by quantitative backscattered electron imaging (qBEI) or ashing reveal the presence of increased mineral. Fourth, at a cellular level, OI bone is almost always high turnover, with increased osteoblasts and osteoclasts. The osteoblasts display delayed differentiation and increased plasticity to adipocytes in culture.

Phenotypic variability, even among patients with the identical mutation, is one of the hallmarks of OI and other skeletal dysplasias and is still poorly understood. Furthermore, this feature obscures attempts to better understand the molecular basis of OI to identify novel target molecules or pathways as the potential basis of improved treatments.

In recent years, the discovery of collagen-related forms of OI led to novel insights into critical pathways involved in bone metabolism. Two of these newly identified causative genes are responsible for dominantly inherited forms of OI—*IFITM5* and *WNT1*. The majority of novel OI types have recessive inheritance of defects (exceptions noted) in genes that are key members of pathways that affect bone mineralization [*IFITM5* (dominant inheritance), *SERPINF1*], collagen modification (*CRTAP*, *LEPRE1*, *PPIB*), collagen processing and cross-linking (*SERPINH1*, *FKBP10*, *PLOD2*, *BMP1*), and osteoblast differentiation and function [*SP7*, *TMEM38B*, *WNT1*, *CREB3L1*, *SPARC*, *MBTPS2* (X-linked inheritance)] (Table 1). Murine OI models have made major contributions to understanding OI pathomechanism in both classical and newly identified types. Recently, zebrafish emerged as an efficient tool in OI phenotyping, with potential for a particular contribution to drug screening studies.

Current pharmacological therapy of pediatric and some adult OI patients involves bisphosphonate (BP) administration, which increases bone mass but does not improve the material properties of OI bone and has equivocal effects on fracture incidence. Teriparatide is an option for adult OI patients with type I OI (1,2), in whom it induces a bone anabolic effect, although increased serum biomarkers of other collagens in addition to type I collagen raise the possibility of a wider alteration in extracellular matrix (ECM) composition (3). Recent studies of other anabolic agents, such as antisclerostin and antitransforming growth factor-beta (anti-TGFβ) antibody, in OI mouse models show improvement in both bone mass and bone strength and may ameliorate the phenotype of OI patients in the future (4).

Collagen Defects and Their Mechanism

Helical Mutations

The most frequent type of mutation found in classical dominant OI results in substitution of one of the glycine residues

that occurs invariably at every third residue along the helical portion of the collagen alpha chain by an amino acid with a bulky or charged side chain. These substitutions disrupt the folding of the collagen triple helical domain (5) (Fig. 1, Table 1). Slow collagen folding in turn leads to overmodification of the collagen helix by enzymes such as lysyl hydroxylase 1 (LH1) and prolyl 4-hydroxylase 1 (P4H1) and, in some cases, to intracellular retention of the misfolded collagen. The enzymes responsible for hydroxylation of proline residues are P4H1, which is critical for triple helical stabilization and which normally modifies about 50% of proline residues in the collagen helical region (6), and prolyl 3-hydroxylase 1 (P3H1), which selectively modifies 1 proline on each alpha chain of type I collagen in bone. Hydroxylation of the P3H1 substrate prolines is important for collagen cross-linking and structural organization in bone (7). Lysyl hydroxylases modify residues in the collagen helix and telopeptide. Many of the hydroxylysine residues are subsequently mono- or diglycosylated. LH1 hydroxylates lysine residues in the triple helical domain, while lysyl hydroxylase 2 functions on C- and N-telopeptides, and lysyl hydroxylase 3 has both hydroxylation and glucosylation activity. Following procollagen processing in the pericellular space, collagen molecules assemble into fibrils. During fibrillogenesis, lysine and hydroxylysine residues in N- and C-telopeptides are oxidatively deaminated by lysyl oxidase, which is a critical step for establishing covalent intra- and intermolecular cross-links in collagen fibrils (Fig. 1A). These cross-links contribute to the mechanical strength of collagen in tissue (8).

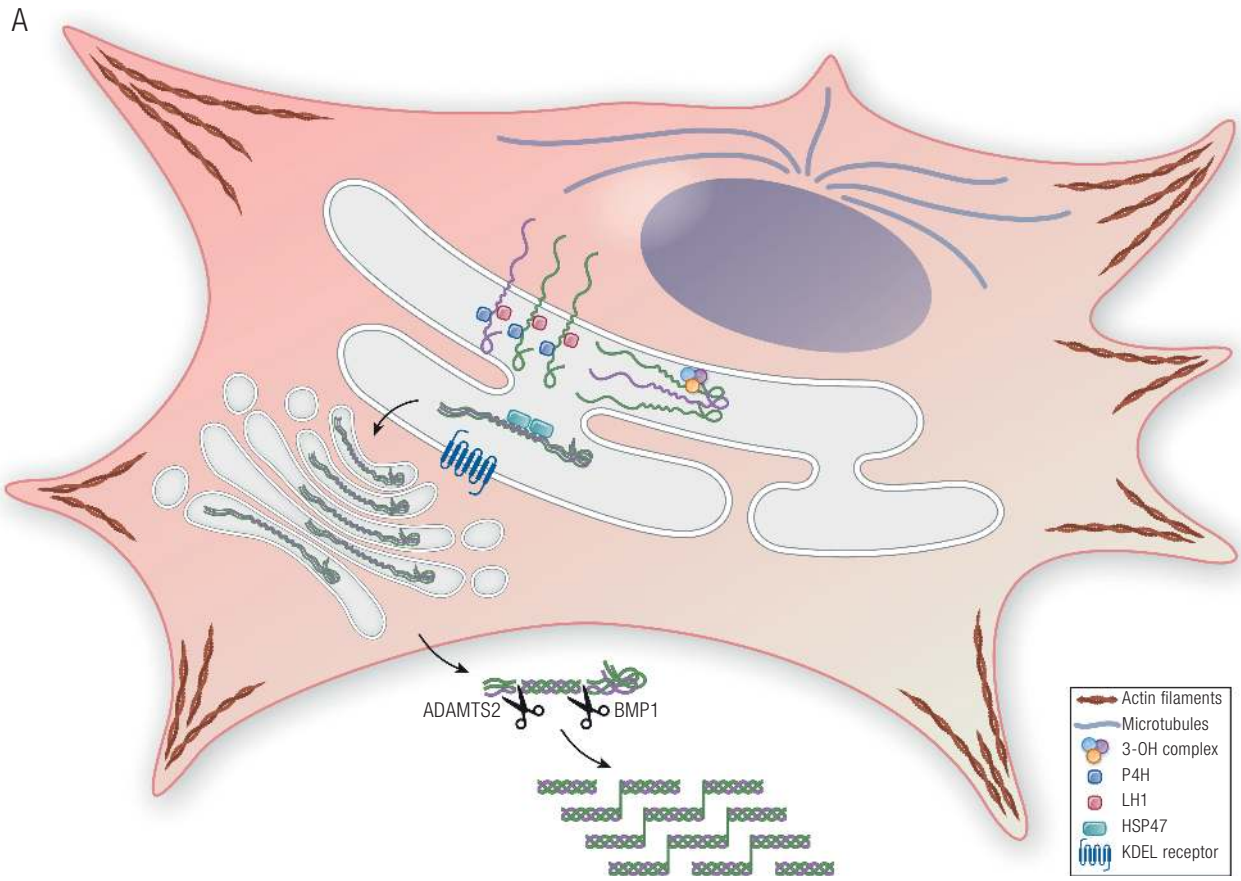

Figure 1. Collagen structure, folding, modification and processing in OI. (A) Procollagen is a heterotrimer consisting of two proα1 (I) and one proα2 (I) chains, which undergo posttranslational modifications of proline and lysine residues during helix folding by prolyl-4-hydroxylase and lysyl hydroxylase 1, respectively. The prolyl 3-OH complex (P3H1, cartilage-associated protein, and peptidylprolyl isomerase B) serves as a folding chaperone; the modification of substrate P986 residue finetunes collagen alignment for cross-linking. The triple helix is further stabilized by Hsp47, an ER chaperone. Once secreted into extracellular space, N- and C-propeptides of procollagen are cleaved by ADAMTS-2 (a disintegrin and metalloproteinase with thrombospondin motifs) and BMP1 enzymes, respectively, and mature type I collagen is released and incorporated into extracellular matrix. A newly discovered OI-causing gene *KDELR2*, encodes KDEL receptor 2 that together with Hsp47 facilitates intracellular recycling of ER-resident proteins. (B) In OI pathophysiology, mutations cause misfolding and overmodification of procollagen chains that may increases protein accumulation in the ER, resulting in ER stress. ER stress causes alterations in cytoskeleton proteins (actin filaments, microtubules), induction of UPR pathways [PERK (especially), inositol requiring enzyme 1, ATF6] to accommodate the chronic stress. For some mutations, ER stress capacity is exceeded, and mutant collagens are labeled with autophagy proteins for lysosomes degradation via microautophagy process at the ER exit sites (ERES). Mutations in *KDELR2* unable binding of Hsp47 to KDEL receptor 2, thus Hsp47 remains bound to collagen molecules extracellularly disrupting collagen fibers formation.

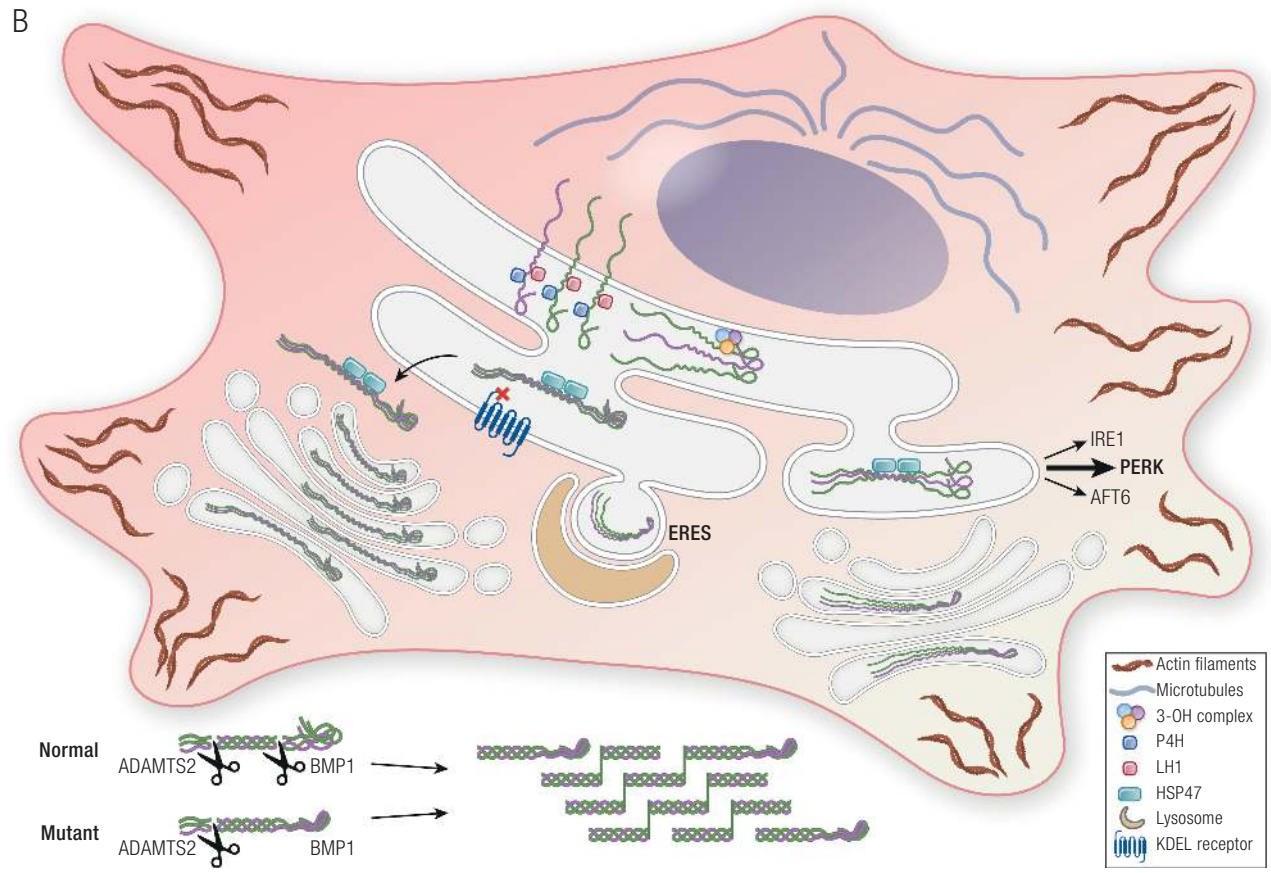

Figure 1. Continued.

How different substitutions lead to the broad range of clinical severity in OI remains incompletely understood. Null mutations in 1 *COL1A1* allele result in quantitative abnormalities of collagen and a fairly uniform mild phenotype that overlaps with osteoporosis. Generally, substitutions of glycine residues to residues with charged or branched side chains have more detrimental effects. Genotype-phenotype modeling indicates that the particular substitution, the chain in which it is located, and its position along the chain all contribute to clinical outcome. Substitutions on the α1(I) chain more often have a severe/lethal outcome than those in α2(I), with the highest concentration of lethal cases in the major ligand binding region on the collagen triple helix. In the α2(I) chain, severe mutations are concentrated in clusters along the length of the chain that correlated with proteoglycan binding site on the higher order collagen fibril. It is clear that clinical severity does not correlate with the extent of collagen overmodification. Slow folding of the helix begins a cascade of events including intracellular and extracellular factors. There is a variable extent of collagen retention in the ER and some ER stress inside the cell, while extracellular factors such as impaired binding of noncollagenous proteins (NCPs), cross-talk with osteoclasts, cell-matrix interactions, and matrix hypermineralization all contribute to pathology. It is currently not possible to predict the clinical outcome of a glycine substitution from first principles, although the previously cited factors and consultation with the Osteogenesis Imperfecta Variant Database (https://oi.gene.le.ac.uk) database of known collagen mutations are useful to learn the range of outcomes for a particular mutation. Collagen structural mutations and the cellular and matrix pathway contributions, as previously cited, have been covered in detail elsewhere.

The Brittle mouse model ($Brtl^{+/-}$), containing an α1(I) Gly349Cys substitution in 1 *COL1A1* allele, has proved to be quite useful for investigating classical OI, as it mimics clinical features of dominant OI and, importantly, shows phenotypic heterogeneity as found among OI patients. One third of $Brtl^{+/-}$ newborn mice die on postnatal day 1 due to respiratory distress, while surviving mice exhibit a moderately severe OI phenotype (9). Comparison of proteomics and cell signaling pathways of these phenotypically distinct mice with an identical mutation reveals potential modifying factors in pathways related to cytoskeletal components, cell stress, energy metabolism, signal transduction, and apoptosis. One of the most surprising findings is that homozygous Brtl/Brtl mice have a normal bone phenotype

compared to Brtl$^{+/-}$ mice (10). One possible cause of rescued bone brittleness and hypermineralization in homozygous mice is the stabilization of essentially all mutant α1(I) collagen chains by disulfide (S-S) bonds formed between cysteines in the same heterotrimer. However, the composition of ECM also differs between heterozygous and homozygous mice, in that all alpha 1 chains are mutant in homozygous mice while heterozygous mice have matrix heterogeneity, with homodimers in 25% of collagen, 1 mutant chain in 50% of collagen, and no mutant chains in 25% of collagen. In addition, there is relative secretory selection in heterozygotes, in which heterotrimers with one mutant chain are partially retained intracellularly, contributing to moderate matrix deficiency (11). It is still unclear which mechanism underlies the rescued phenotype in homozygous Brtl mice.

ER Stress, Cytoskeletal Changes

Collagen, the most abundant protein in the ECM, is initially synthesized as procollagen chains that are transported to the endoplasmic reticulum (ER) for posttranslational modification and proper folding before release to the extracellular space. Improperly folded collagen is often secreted more slowly from cells or may be partially retained in the ER. Retention of mutant collagen triggers induction of pathways that are necessary for the cell to manage the stress caused by accumulation of misfolded protein (Fig. 1B). Published studies point to the difficulty of determining whether these pathways modify the phenotypic outcome for the identical mutation. In skin cells of lethal Brtl$^{+/-}$ mice, galentin-7, associated with apoptosis and proteasomes are increased, while maspin, involved in cell-matrix interactions, was reduced compared to both surviving Brtl$^{+/-}$ and wild-type (WT) pups. However, the levels of maspin and proteasomes in calvarial bone of lethal pups relative to WT and surviving mutant mice were opposite to those found in skin (12). In calvarial osteoblasts of lethal mice, increased expression and protein levels of ER stress-related protein growth arrest- and DNA damage-inducible gene 153/Chop again points to difficulty managing ER stress and impeding apoptosis (13). Even with a focus on bone studies, differences in bone type throughout the skeleton will necessitate validation of calvarial bone as a surrogate for axial long bones.

ER stress could potentially affect cell survival by disrupting the cytoskeleton organization (Fig. 1B). The cytoskeleton is a dynamic network of 3 main sets of proteins—intermediate filaments, microtubules, and actin filaments—involved in maintenance of cell integrity by regulating cell shape and mechanics under applied extracellular forces. Changes in expression of cytoskeletal components are found in lethal Brtl$^{+/-}$ mice. Vimentin, which has a crucial role in cell integrity as an intermediate filament, is reduced in bone and skin cells from lethal mice (12). The microtubule component stathmin and actin filament cofilin-1 play roles in cytoskeletal dynamics by depolymerizing of microtubules and actin filaments, respectively. Both stathmin and cofilin-1 are increased in bone, skin, and lungs of lethal Brtl$^{+/-}$ mice, raising the possibility that these factors contribute to respiratory distress in nonsurviving mice. The cytoskeleton also plays an important role in cell proliferation and differentiation, potentially contributing to reduced deposition of bone collagen. Moreover, in 2 pairs of patients who had identical collagen mutations but divergent phenotypic outcomes of lethal types II or severe type III OI, cytoskeletal disruption was demonstrated in fibroblasts from the 2 lethal, but not the 2 severe, OI patients, suggesting that further investigating the role of the cytoskeleton in the variability of OI phenotypic severity at the bone level is warranted (14).

Misfolded protein accumulation in the ER activates the unfolded protein response (UPR) and its 3 pathways regulating ER-resident signaling components: inositol requiring enzyme 1 (IRE1), eukaryotic translation initiation factor 2 alpha kinase 3 (PERK), and activating transcription factor 6 (ATF6) (Fig. 1B). Old astrocyte specifically induced-substance (OASIS), a member of 3′,5′-cyclic adenosine 5′-monophosphate (cAMP) responsive element-binding (CREB)/activating transcription factor family, shares similar structure with ATF6 (15). It was shown in osteoblasts-like cell line overexpressing OASIS that, once exposed to ER stress, OASIS is cleaved and translocated in the nucleus (15). However, it is not clear whether OASIS provides an alternative pathway in the instance of collagen misfolding. In cells of OI patients, UPR PERK and IRE1 pathways are evidently upregulated as a response to mutant collagen misfolding or retention in the ER. However, if the UPR exceeds its capacity to restore function of misfolded proteins, another protective mechanism, autophagy, is activated. Autophagy is a lysosomal self-digestion pathway that contributes to the maintenance of cell homeostasis by removal of damaged cell components. One of the most common marker genes used in detection of autophagy, microtubule-associated protein 1A/1B-light chain 3 (LC3-II), contributes to formation of the autolysosome and is elevated in OI patient fibroblasts, which also express higher levels of cleaved caspase 3 and annexin V, markers of apoptosis. The application of chemical chaperone 4-phenylbutyric acid (4-PBA) to fibroblasts of OI patients, potentially facilitating collagen folding to increase collagen secretion, increased general protein secretion and autophagy (16).

The extent to which ER stress and the UPR contribute to the severity of the OI phenotype remains a controversial

topic that merits additional investigation. The moderate UPR pathway changes, and some degree of ER swelling on electron microscopy images in cells with collagen structural defects is also consistent with an adaptive response but is not necessarily the driver of bone pathology. It is worth noting that in type XIV OI, in which the absence of transmembrane protein 38B (TMEM38B) triggers ER stress along the same calcium transport system routinely used experimentally in a wide array of cellular systems to induce ER stress, that the OI skeletal phenotype is mild to moderate in severity (see also section on TMEM38B defects). Even in classical OI with collagen structural defects, many collagen mutations do not result in ER retention of collagen. The extent to which mutant collagen is retained and/or general protein secretion is decreased needs examination in more phenotypically relevant cells, osteoblasts and osteocytes. Osteoblasts have been available almost entirely from murine models; detailed studies in patient osteoblasts and relevant controls are lacking. Effects on cellular differentiation, such as those caused by ER stress, are important but could also be influenced by cell matrix and collagen-NCP interactions, since the OI bone matrix contains not only mutant collagen but also abnormal proportions of NCPs. Murine bone matrix containing only mutant collagen, such as Brtl/Brtl or Brtl/mov mice, have a milder or near normal phenotype, supporting the importance of matrix composition. The hypermineralization of mutant matrix, in addition to its quantity, is critical to the brittleness of OI bone and has not been connected directly to ER stress. Fortunately, murine models provide easy access to bone to explore the relative contributions of ER stress, general protein secretion, matrix composition, and cell-matrix interactions prior to their validation in patient bone samples.

Another OI murine model that shows involvement of ER stress as a contribution to mechanism is a mouse with a Gly610 to cysteine substitution in the triple helical domain of the collagen α2(I) chain. This mouse exhibits mild to moderately severe OI in heterozygotes and perinatal lethal OI in homozygotes. Due to intracellular accumulation of misfolded procollagen, there is induction of nonconventional UPR in osteoblasts with increased phosphorylation of eukaryotic initiation factor 2α (EIF2α) but with no change in expression of UPR components heat shock protein family A (Hsp70) member 5 (BiP) and spliced X-box binding protein 1 (Xbp1). Osteoblasts show reduced mineralization with lower expression of osteoblasts differentiation marker genes (17). Recently, a noncanonical autophagy route that may contribute to OI pathophysiology was identified in osteoblasts from the *COL1A2* G610C mice. Using live-cell microscopy, it was found that mutant collagen at ER exit sites (ERESs) is labeled with autophagy proteins for lysosomal degradation through a microautophagy-like mechanism that can remove excess procollagen from cells (18) (Fig. 1B). When autophagy is induced, osteoblasts achieve reduction in accumulation of misfolded procollagen and improvement of collagen matrix deposition (17). Additionally, these mice have induced ER stress in hypertrophic chondrocytes of growth plate, causing growth plate abnormalities and, consequently, growth deficiency (19). However, therapeutic induction of autophagy for OI treatment, however, was not supported by results from α2(I)G610C OI mice that were administered rapamycin to promote autophagy. Although trabecular bone mass was improved by rapamycin treatment in the α2(I)G610C OI mouse, bone mechanical properties were not rescued, and bone brittleness and growth were actually worsened (20). While these off-target effects of rapamycin represent a significant limitation, a different approach of stimulating autophagy could be more effective in rescuing OI bone phenotype.

One common feature for OI patients is reduced muscle strength; however, it is unknown whether it reflects muscle pathology or decreased physical activity. G610C mice show that hindlimb muscles strength is comparable to WT, and mice were able to complete an 8-week treadmill regimen. The exercises did improve bone stiffness; however, other biomechanical properties remained unchanged (21). G610C mice bred on different backgrounds show alterations in bone structure and geometry, making this model a useful tool in exploring different genetic factors that could potentially modify the bone phenotype (22).

Z-Fish Models

Zebrafish models of OI have recently emerged as an additional tool for investigating the molecular basis of OI phenotypic variability. Characteristics including lower-cost maintenance, short developmental time, ease of mutation induction, small size, and large offspring number make zebrafish models useful in drug screening studies that would require considerably more time if conducted in mice. However, although osteogenesis is highly conserved, the structure of type I collagen in zebrafish models is different than mammals and consists of α1, α3, and α2 chains encoded by *col1a1a, col1a1b*, and *col1a2* genes, respectively (23).

The zebrafish *Chihuahua* (Chi/+) model with a helical defect in type I collagen carries a heterozygous single nucleotide mutation causing a typical glycine substitution (G574D) in the α1(I) chain of type I collagen. It strongly reproduces the phenotypic features of dominant OI (24). Chi/+ mutants show growth delay and rib fractures, as well as vertebral compressions similar to OI patients. Interestingly, while murine OI models do not have

spontaneous vertebral compressions, zebrafish showed fused and misshapen vertebrae. Whether these vertebral anomalies have a comparable etiology to vertebral compressions in patients due to mechanical loading remains to be demonstrated (25).

Low bone quality as well as a low BFR contribute to Chi/+ skeletal deformities. At the cellular level, Chi/+ fish have intracellular retention of mutant collagen and ER enlargement. Heat shock protein 47 (Hsp47), a collagen-specific chaperone that binds to and stabilizes the folded configuration of procollagen to prevent unfolding or aggregation to facilitate its secretion, was shown by whole-mount immunostaining to be expressed at a higher level in mutant tail fin fold, skin, and intersomitic space compared to WT. The increased expression of Hsp47 could be a result of its effort to facilitate synthesis and secretion of collagen (25). At the bone tissue level, nanoindentation revealed reduced bone stiffness and toughness. Fourier transform infrared spectroscopy (FTIR) identified reduced collagen maturity and mineral crystallinity in Chi/+ fish, additionally affecting bone material quality. Finally, OI zebrafish bone quality reflects impaired mineralization, with increased mean calcium concentration (CaMean) by qBEI, as in OI patients (26). OI zebrafish models with different mutations in collagen type I show a broad range of skeletal phenotype, which is most likely due to intergenotype variability as seen in OI patients. Study of these models may contribute to better understanding of mechanisms underlying OI phenotypic variability (27).

C-Pro Cleavage Site and Bone Morphogenetic Protein Defects

Cleavage site defects and hypermineralization

Type I collagen is synthesized as the promolecule, procollagen, consisting of the collagen triple helical domain plus both N- and C-propeptides. Following synthesis, 2 proα1 and 1 proα2 chains align with each another at the C-propeptide and initiate association and folding toward the N-terminus. The resulting procollagen heterotrimer is secreted into the pericellular space. To release mature collagen molecules required for formation of collagen fibrils, N- and C-propeptides are each enzymatically processed by a specific metalloproteinase, a disintegrin and metalloproteinase with thrombospondin motif 2 (ADAMTS-2) and bone morphogenetic protein 1 (BMP1)/tolloid-like proteinases, respectively (Fig. 1A).

Impaired C-propeptide processing was first described in 2 children with substitutions in residues comprising the cleavage site, proα1(I) p.Asp1219Asn and proα2(I) p.Ala1119Thr, respectively. They had dominantly inherited OI with relatively mild OI symptoms and a paradoxically

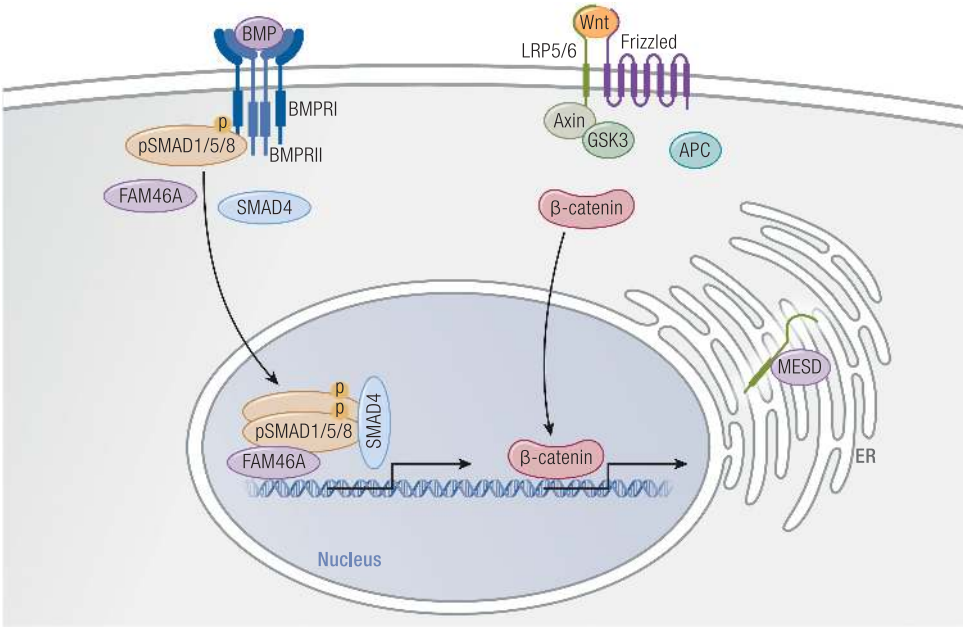

Figure 2. Wnt and Bmp signaling pathways disrupted in osteogenesis imperfecta. (Left) BMP ligand binds to BMPRI and BMPRII receptors and induces phosphorylation of SMAD 1/5/8. Terminal nucleotidyltransferase 5A (FAM46A) binds to phosphorylated SMAD 1/5/8 and protects it from ubiquitination. Together SMAD 1/5/8, FAM46A, and SMAD4 form a complex that translocates to the nucleus where it induces transcription of BMP target genes. (Right) Wnt signaling is activated by binding of WNT1 ligand to the Frizzled receptor and LRP5/6 co-receptors, which stabilizes β-catenin levels by inhibiting the degradation complex consisting of axin, adenomatous polyposis coli (APC), and glycogen synthase kinase 3 (GSK3). Subsequently, β-catenin migrates to the nucleus where it activates transcription of Wnt target genes. The recently proposed causative gene for OI, MESD, is an ER chaperone that facilitates maturation and trafficking of LRP5/6 co-receptors.

high bone mass on DXA. Their high bone mass is characterized by increased bone mineralization on qBEI, as well as increased mineral-to-matrix ratio on FTIR spectroscopy. Histomorphometry revealed increased osteoid seams, elevated BFR and increased TbN in the child with proα1(I) substitution, due to inefficient cleavage of 2 proα1(I) chains. In contrast, in the patient with a proα2(I) substitution, proα1(I) chains are mostly cleaved and thinner osteoid seams were found, along with elevated TbN (28). A subsequent study demonstrated the same findings in a broader age range (2.5-75 years old) of patients with similar mutations (29). These data supported a critical, and previously unappreciated, role for C-propeptide cleavage in bone mineralization. The mechanism of high bone mass OI is currently under investigation in a murine model.

BMP1 defects in patients and mice

BMP1 was first discovered in bone extracts based on its ability to induce ectopic bone formation (30) (Table 1). There are 4 BMP1-like proteinases: BMP1 and its alternative splice variant mammalian tolloid (mTLD) encoded by the same gene, *Bmp1,* and mammalian tolloid-like 1 and 2 (mTLL-1 and mTLL-2, respectively). The main role of BMP1 like proteinases involves its procollagen C-proteinase (pCP) activity, which is responsible for cleavage of C-terminal propeptides from procollagens types I, II, and III (31-33). Other functions involve processing of small leucine-rich proteoglycans (decorin, biglycan, and osteoglycin) (34-36); activation of lysyl oxidases, an enzyme important for cross-linking of collagen molecules (37); processing of dentin matrix protein 1 (DMP1) required for bone mineralization (38); and activation of TGFβ1, one of the major signaling molecules for bone remodeling (39).

Homozygous *Bmp1* null mice die during embryonic development due to failure of ventral body wall closure, whereas embryonic lethality of homozygous *Tll1* mice is caused by cardiovascular defects (40,41). Conditional knockdown of *Bmp1* and *Tll1* (BT^{KO}) has been created by inducing postnatal ablation of both genes to create surviving double homozygous mice. BT^{KO} mice have increased bone fractures and brittleness, with reduction of cortical and trabecular BV/TV, and increased osteoid seams. The bones are highly remodeled, consistent with increased osteoblast and osteoclast number. Osteocytes show decreased maturation with reduced sclerostin and abnormal cell morphology. *Bmp1*-null or *Bmp1*/*Tll1* null embryos have "barbed-wire" collagen fibrils with barb-like projections on fibril surfaces indicative of incorporation of pC-collagen (42).

Children with homozygous or compound heterozygous mutations in *BMP1* range in phenotype from mild to severe. In most cases, the impaired processing of the type I procollagen C-propeptide leads to high bone mass OI and abnormal organization of collagen fibrils (43-45) (Fig. 1B). High bone mass in this context refers to results of bone densitometry studies, with Z scores of up to +3 compared to normal population and high bone matrix mineralization shown by bone mineral density distribution (BMDD) analysis, rather than the elevation of BV/TV that is found in other high bone mass situations. The administration of BPs to patients with high bone mass may increase bone stiffness and brittleness.

Adult patients with autosomal recessive OI due to novel heterozygous missense and frameshift mutations in *BMP1* have short stature, frequent fractures, and rhizomelic shortening of long bones. In patient fibroblasts, processing of procollagen as well as prodecorin, important for collagen fibrillogenesis, were defective. Immunofluorescent staining revealed impaired collagen assembly in vitro. Fibrils in dermal ECM were irregular and intrafibrillar spaces were filled with amorphous deposits on electron microscopy (46).

Defects in modulator of bone morphogenetic protein signaling

The bone morphogenetic protein (BMP)/TGFβ signaling pathway, distinct from the BMP procollagen processing function, may also be contributory to OI syndromes. *FAM46A* is a member of the superfamily of nucleotidyltransferase fold proteins, whose functions are largely unknown (47). In Xenopus development, Fam46a physically interacts with SMAD family member 1/SMAD family member 4 and is a positive modulator for induction of BMP-target gene transcription (48) (Fig. 2, Table 1). *FAM46A* is expressed strongly in murine fetal skeleton and in human osteoblasts indicating a possible role in bone development (49,50). *FAM46A* variants have been previously associated with autosomal recessive retinitis pigmentosa (51). Interestingly, homozygous mutations in *FAM46A*, detected in children originally thought to have Stüve-Wiedemann syndrome, have been reported to cause a severe form of autosomal recessive OI diagnosed in the first years of life, with congenital bowing of lower limbs, fractures, dental abnormalities, and blue sclerae (50). Further confirmation of these mutations as OI-causative await fibroblast biochemical studies and bone tissue analyses. An *N*-ethyl-*N*-nitrosourea (ENU)–induced mouse model for recessive defect in FAM46A has elevated serum alkaline phosphatase, small size, and fragile bones with reduced trabecular volume and cortical thickness (49).

Defects in the C-propeptide

The C-propeptide of procollagen type I is critical for chain recognition and association. Although mutations in this region are not incorporated into the ECM, they cause OI with

phenotype severity from mild to lethal. Both premature termination codons (PTCs) and amino acid substitutions have been reported. The severity of OI caused by C-propeptide defects is influenced by the PTC location. When the PTC leads to nonsense-mediated messenger RNA decay (NMD), the production of mutant proα1 (I)-collagen chains is reduced and OI outcome is milder; the absence of NMD leads to incorporation of mutant chains into procollagen, which affects both folding and overmodification of procollagen, leading to a severe or lethal OI phenotype (52).

Now, the crystal structure of C-propeptide trimer from human procollagen III heterotrimer (CPIII) provides a more reliable tool for predicting OI severity. The C-propeptide is flower-shaped and consists of a stalk, a base, and 3 pedals. C-propeptide mutations resulting in mild to moderate OI phenotypes often involve surface-located residues in the regions not participating in interchain interactions, which makes them unlikely to interfere with folding or trimerization. Mutations with more severe and lethal outcomes are located near C-terminus, at the interface between the petal and the base. Mutations in this region are involved in intrachain disulfide bonding, interchain interactions, or stabilization of the hydrophobic core. The structural model of the C-propeptide can be seen in prior studies (52-54). The intrachain disulfide bonds are important for initial stages of collagen assembly. Mutations affecting disulfide bonds delay chain association and secretion of mutant chains (55). New evidence shows that the proteostasis network engages directly with the misfolded mutant C-pro domain, determining secretion *vs* retention of procollagen. Retained mutants are targeted to ER-associated degradation (56).

Patient fibroblasts with C-propeptide structural defects exhibit increased levels of BiP, an ER chaperone, which may be a response to retention of mutant procollagen in the ER and ER stress (57). BiP has been shown by coimmunoprecipitation to bind directly to abnormal procollagen in OI fibroblasts but not in control cells (58). C-propeptide mutations, which disrupt trimer assembly, induce degradation of procollagen chains via the proteasomal ER-associated degradation pathway (59). However, the importance of ER stress in OI caused by C-propeptide mutations remains unclear. Recent findings indicate that C-propeptide defects in OI patients induce mislocalization of procollagen in the ER lumen *vs* the normal location at the ER membrane, which may limit exposure of the chains to enzymes involved in posttranslational modification. Moreover, cleavage of the propeptide is impaired both in the pericellular space and in vitro, suggesting that the mutations indirectly disturb the 3D structure of the cleavage site (54).

The Aga2 mouse is an ENU-induced mouse model affecting the C-propeptide region of type I collagen. The induced mutation is a novel T to A transversion within intron 50 of *Col1a1*, which generates a novel exon 39 splice acceptor site, ultimately leading to a frameshift with a predicted termination codon beyond the endogenous stop. Mice show severe to lethal phenotypes with increased bone fractures and decreased bone mass. Intracellular accumulation of misfolded collagen induces ER stress with upregulation of BiP, Hsp47, and growth arrest- and DNA damage-inducible gene Gadd153/Chop, as well as activation of caspase-3 and -12 and apoptosis of osteoblasts (60). Aga2 perinatal lethal mouse show cardiac and pulmonary defects due to reduction in collagen and loss of ECM integrity. These results are validated in a pediatric OI patient cohort with types III and IV (61) (see also the section on treatment approaches to OI).

Types V and VI OI

Type V Patients and Mice

Type V OI is caused by a recurrent autosomal dominant mutation in the 5'-UTR of the interferon induced transmembrane protein 5 (IFITM5), encoding bone-restricted interferon-induced transmembrane protein-like protein (BRIL) (62,63) (Fig. 3, Table 1). BRIL is localized to the osteoblast plasma membrane, although it is also expressed to a lesser extent in fibroblasts. The IFITM5 c.-14C>T mutation creates a new start codon, resulting in addition of 5 residues (MALEP) to the cytoplasmic N- terminus of BRIL. The BRIL MALEP mutation is distinctive among OI types, both as the only disease-causing mutation located on the 5'-UTR and for creating a new start codon upstream of the normal translation start (62). BRIL is attached to the cell membrane on the cytoplasmic side by palmitoylation of cysteines 50 and 51 (64). BRIL is also known to interact with FKBP prolyl isomerase 11 (FKBP11) on or within the extracellular face of the plasma membrane. Binding of BRIL to FKBP11 interferes with the interaction of cluster of differentiation 9 (CD9) with cluster of differentiation 81 (CD81)-FKBP11 complex, which, in turn, regulates the expression of interferon-induced genes. These interactions may connect the immune system to OI type V pathophysiology (65).

OI type V was first delineated clinically in 2000 by Glorieux et al as a dominantly inherited condition that was not associated with a mutation in type I collagen (66). It is generally a moderate form of OI, similar in severity to type IV OI, although height and bone mineral density vary widely. A triad of findings were first noted: (1) history of formation of hyperplastic callus after fractures or following surgery; (2) calcification of the interosseous membrane of the forearm; and (3) a hyperdense metaphyseal

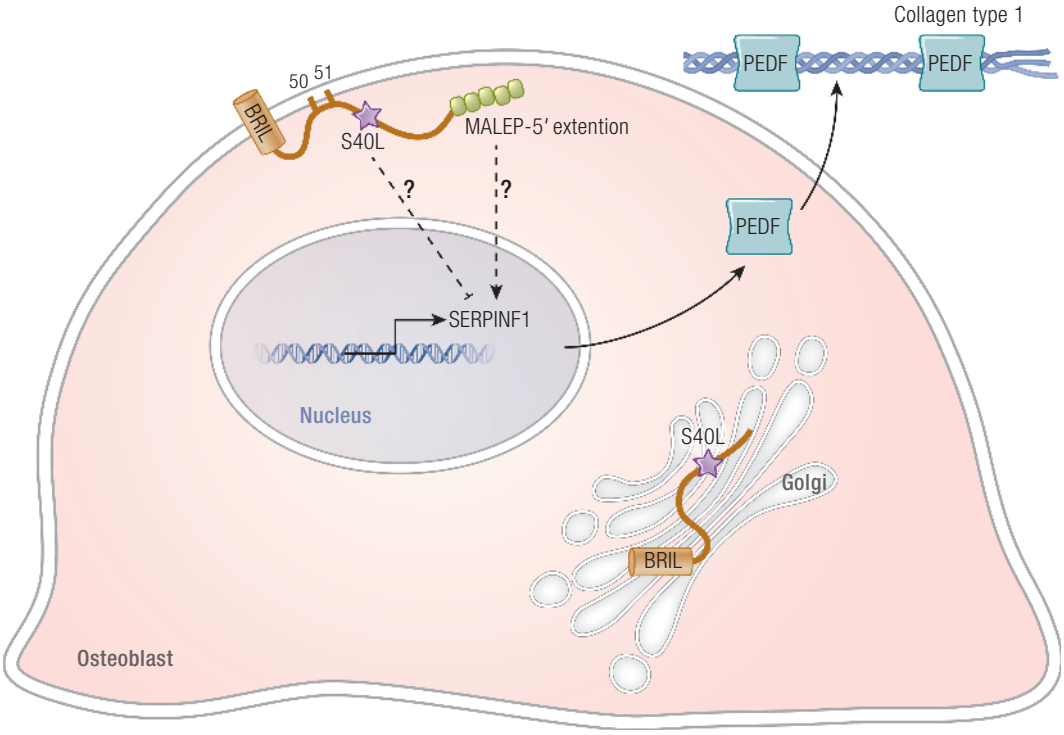

Figure 3. Defects in BRIL and PEDF, altering bone mineralization, cause OI. BRIL has an important role in the regulation of *SERPINF1* transcription in the nuclei and resultant production of the protein PEDF. In a normal osteoblast, BRIL is attached to the cell membrane by palmytoilation sites. In the mutation causing Type V OI, 5 aa resides are added to the 5′ end of BRIL. This in turn increases the transcription of *SERPINF1* and its protein PEDF. In the presence of a BRIL Serine40Leucine substitution, the palmytoilation process is impaired, and BRIL is trapped in the Golgi apparatus. Clinically, BRIL S40L patients have features of severe type VI OI (type atypical VI OI) rather than type V OI. PEDF binding to collagen in matrix is critical for its anti-angiogenic function. Osteoid is increased in PEDF null bone tissue by an unknown mechanism.

band in the forearm that develops even in infants. Radial head dislocations are also a frequent finding. Examination of bone from type V patients under polarized light reveals a mesh-like pattern of lamellation in essentially all patients. There is a striking variability of phenotype among patients with type V OI, in terms of combinations of characteristic clinical and radiographic findings. Hyperplastic callus or scoliosis are present in about 2/3 of cases, while most patients have radial head dislocation and ossification of the interosseous membrane. Patients do not exhibit blue sclera or dentinogenesis imperfecta (62,66,67). Some patients are not suspected of having type V OI prior to DNA sequencing.

The hypertrophic callus and dense metaphyseal bands of type V OI, as well as the mutation structure with elongation at the N-terminus of the protein, suggested that the causative BRIL mutation results in a gain of function (62,68) (Fig. 3). The elongated BRIL protein is stable in cells but does not display changes in topology, palmitoylation, or membrane localization, all providing additional evidence that the type V OI mutation is gain of function (68). Osteoblasts from patient bone samples cultured in vitro exhibit increased levels of transcripts for osteoblast maturation markers such as osteopontin (secreted phosphoprotein 1), alkaline phosphatase (ALPL), and integrin-binding sialoprotein (IBSP), suggestive of alteration of middle stages of differentiation (69). These data are in agreement with elevation of patient serum alkaline phosphatase levels during active hyperplastic callus formation (66), and chronically in some patients (70).

Bone tissue in type V OI patients is highly mineralized on qBEI, similar to classical collagen-based OI (71). As in collagen-based OI, trabecular bone mass (BV/TV) is decreased in type V OI bone, while BFR, usually elevated in collagen-based OI, is decreased in iliac crest biopsies of type V OI (66). Type V OI bone also has a striking increase of osteocyte number and size (71). These data pose a paradox between the expected low BV of trabecular bone in type V OI and the exuberant extraosseous bone formation of hypertrophic callus and interosseous membrane calcification. Since the exuberant ossification involves the outer surface of bone, it has been speculated that it represents dysregulated periosteal proliferation that simply uses the extraosseous structures as a guide (67). Alternatively,

the BRIL mutation may impair formation of orderly lamellar bone during remodeling, as the same configuration as type V exuberant bone is seen in periosteal bone apposition during normal skeletal development (71). Further investigation of patient osteoblasts and murine models may illuminate the mechanism of the BRIL MALEP mutation at osseous and extraosseous sites.

IFITM5 knock-out (KO) mice do not display a skeletal dysplasia. However, mice in which the corresponding BRIL mutation was introduced by clustered regularly interspaced short palindromic repeats (CRISPR) are embryonic lethal. These pups showed skeletal deformities, including wavy ribs, bent long bones, and hypermineralized skulls (72). Interestingly, their long bones were filed with hypertrophic chondrocytes (72).

Type VI and Atypical VI OI Patients and Murine Models

Type VI OI is a severe recessive bone dysplasia caused by mutations in Serpin family F member 1 (SERPINF1). SERPINF1 encodes pigment epithelium-derived factor (PEDF), a 50 kDA secreted glycoprotein, which was already well-known as a potent antiangiogenic factor (Table 1). In type VI OI, the causative mutations are generally null mutations and result in an absence of serum PEDF that is unique to this type. PEDF is known to bind to type I collagen and it is intriguing that mutating residues on PEDF that are critical to collagen binding abrogates its anti-angiogenic effect (73) (Fig. 3). In cultured osteoblasts, addition of PEDF reduced expression of sclerostin (SOST) in a dose-dependent manner, which contributes to the osteogenic effect of PEDF, and suppressed expression of genes associated with osteocytes in bone tissue, including SOST, matrix extracellular phosphoglycoprotein (MEPE), and DMP1 (74). In addition, PEDF is highly expressed in adipocytes where its role in adipogenesis is inhibitory; conversely, PEDF expression is decreased during adipogenesis (75). The PEDF KO mouse has a 50% increase in total body adiposity (75). PEDF binds to adipose triglyceride lipase (ATGL), suppresses peroxisome proliferator-activated receptor gamma (PPARγ), and, consequently, platelet glycoprotein 4 (CD36), itself a fatty acid–trafficking protein (76). Overall, PEDF increases osteogenesis and inhibits adipogenesis, consistently favoring differentiation of mesenchymal stem cells into osteoblasts *vs* adipocytes (75).

Type VI OI was first delineated in 2002, with recessive inheritance of a severe bone dysplasia resembling type III OI. Distinct from type III OI, type VI patients are generally not identified at birth but present with frequent fractures after 1 year of age (77). Other unique clinical identifiers for type VI OI include persistently elevated alkaline phosphatase in childhood and absence of serum PEDF. The bone tissue of type VI OI is also distinctive; the combination of increased unmineralized osteoid and fish-scale lamellae under polarized light was critical to the original clinical delineation (77).

The *SERPINF1*$^{-/-}$ null mouse model is characterized by reduced BV/TV and elevated osteoid, as found in clinical type VI OI (78). In vitro, mineral deposition was increased and the mineral to matrix ratio was elevated in calcified nodules (78). Treatment studies involving this mouse yielded conflicting results. Delivery of PEDF via helper-dependent adenoviral vector injection into the tail vein of 2-month-old *SERPINF1*$^{-/-}$ mice did not improve bone phenotype (79). In contrast, intraperitoneal injection of PEDF-containing microspheres into 19-day- and 6-month-old *SERPINF1*$^{-/-}$ mice was reported to improved bone mass and mechanics (80). The different outcomes may reflect the different PEDF modes or sites of delivery, local *vs* liver production of PEDF, or ages of treated mice. Replacement therapies will need to be further investigated to validate the best treatment option.

IFITM5/BRIL S40L (c.119 C>T) is a special mutation that occurs in the gene causing type V OI but results in a pattern of OI findings that resembles type VI OI (Fig. 3, Table 1). The index patient with this mutation has bone dysplasia more severe than even typical type VI OI, elevated serum alkaline phosphatase in childhood that returned to normal at skeletal maturity, and a fish-scale lamellar pattern with appearance similar to fish scales rather than normal appearance of parallel lines when bone was viewed under polarized light (81). Serum PEDF was normal but cultured fibroblasts and osteoblasts had nearly absent secretion of PEDF. This patient, and the additional 8 independent patients reported with the same mutation (81-88), do not have the distinctive clinical and radiographic findings of type V OI. Both the S40L substitution of atypical type VI OI and the MALEP insertion of type V OI are heterozygous, supporting dominant inheritance of the de novo mutation. The S40L BRIL mutation occurs near the palmitoylation sites at S50 and S51 (64) (Fig. 3). In mouse, the corresponding mutation occurs at S42, and substitution with leucine leads to poor palmitoylation of BRIL at S52 and S53 and its entrapment in the Golgi (68). Differentiation of osteoblasts in vitro from type V OI and BRIL S40L patients shows a reciprocal relationship between these mutations: cells with the MALEP mutation have increased mineralization in culture, as well as increased *SERPINF1* expression and PEDF secretion, while osteoblasts with S40L have reduced mineralization in culture and reduced SERPINF1 expression and PEDF secretion. Interestingly, both mutations result in reduced

collagen expression during osteoblast differentiation (69,81).

A murine model for atypical type VI OI was recently generated with an *Ifitm5* S42L mutation. This is a dominant mutation, as in the patients, and mice exhibit a mutation dosage effect. Heterozygous mice have fractures and reduced DXA compared to their WT littermates, and homozygous mice display a more severe phenotype (89).

The mechanism of the implied connection between BRIL and PEDF generated by the *IFITM5* S40L substitution is unclear. BRIL and PEDF do not interact directly with each other, and neither has a function related directly to collagen processing, synthesis, folding, or cross-linking, although each affects osteoblast mineralization and differentiation in a complementary way.

Type XIV OI—TMEM38B Defects

Calcium Flux Defect in a Distinctive OI Form

Calcium signaling is important for the body; release of calcium from the sarcoplasmic reticulum (SR) and ER is crucial for diverse cellular roles (90). The process involves 2 key activities: calcium release that creates counter movement of ions across SR/ER to stabilize the transport of negative potential on the luminal side and calcium movement from intracellular stores through calcium release channels to the plasma membrane (91,92) (Fig. 4). Ca^{2+} acts as a secondary messenger and interacts with many proteins, among which is type I collagen. The role of Ca^{2+} in collagen metabolism is both direct, in that Ca^{2+} binds to the procollagen C-propeptide and stabilizes the disulfide bonds and interchain hydrogen bonds essential for procollagen

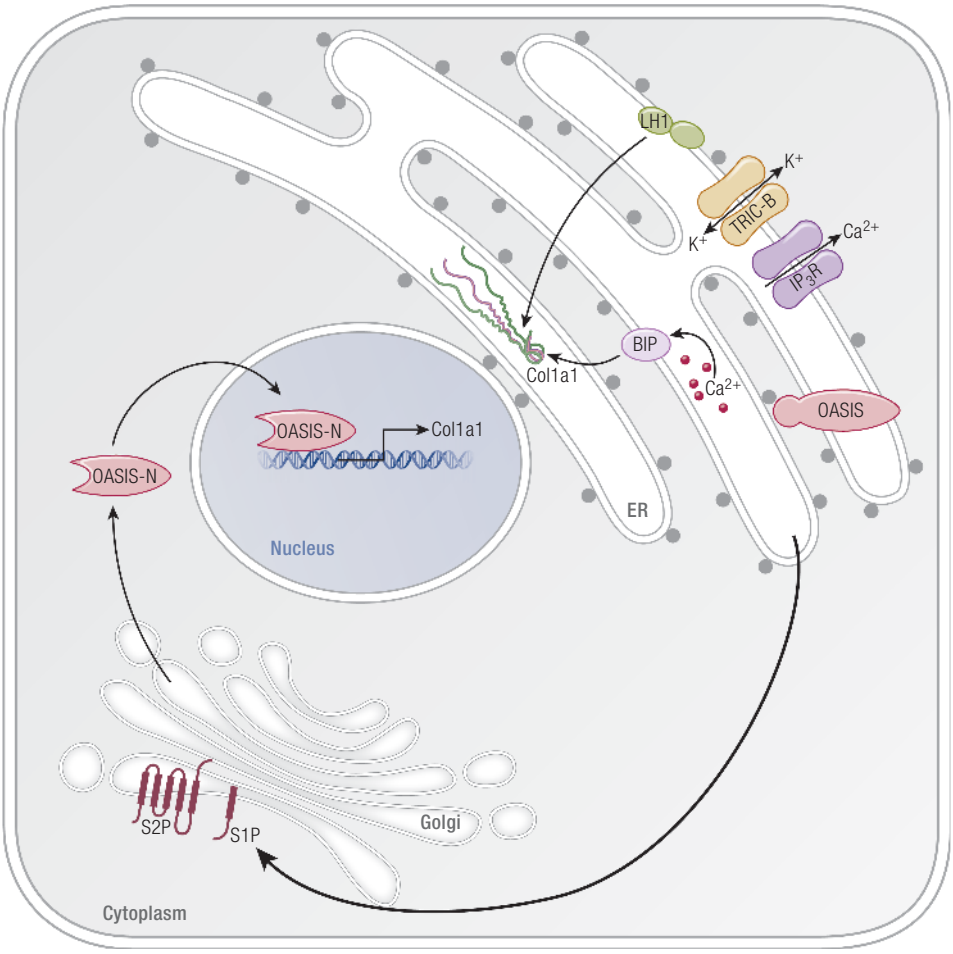

Figure 4. OASIS, RIP, and TRIC-B role in bone formation. The ER serves as a major storage site for intracellular Ca^{+2}. Type I collagen is synthesized within this compartment and Ca^{+2} is a cofactor for many enzymes involved in collagen folding and modification. Upon receiving extracellular stimuli, the ER lumen releases Ca^{+2} to the cytoplasm through IP_3R. TRIC-B is involved indirectly in the kinetics of Ca^{+2} entry and released from the ER by mediating K+ flux; this maintains the electroneutrality through the ER membrane. When TRIC-B is deficient, altered Ca flux interferes with multiple Ca^{+2} binding chaperones such as BiP and modifying enzymes such as LH1, thus disrupting the synthesis and secretion of collagen. Subsequent to cell stress, regulatory proteins in the ER membrane, such as OASIS, are transported from the ER to the Golgi membrane for RIP. After sequential cleavage by S1P and S2P, transmembrane proteases in the Golgi, the released N-terminal portion of OASIS can then translocate into the nucleus and activate transcription of a set of matrix-related genes, including collagen type I alpha/alpha 21 chain.

trimerization and folding (53), and indirect, in that Ca^{2+} is a critical cofactor for multiple enzymes involved in procollagen posttranslational modification.

Yazawa et al reported the discovery of 2 trimeric intracellular cation (TRIC) channels which are differentially expressed on intracellular membranes and have roles as counter ion channels in synchrony with ryanodine receptor/inositol 1,4,5-trisphosphate (RyR/IP3)–mediated Ca^{+2} release (93) (Table 1). The ER membrane is rich in TRIC channels (94). TRIC-A is encoded by *TMEM38A* and is expressed in the SR of muscle cells, including cardiac muscle, and functions coordinately with ryanodine receptor-mediated Ca^{2+} release. TRIC-B, encoded by *TMEM38B*, is ubiquitously expressed in the ER and operates in synchrony with inositol 1,4,5-trisphosphate receptor (IP_3R) (93,95,96) (Fig. 4). TRIC-A and TRIC-B are coexpressed in many tissues, including the heart, and may overlap in some functions, making it difficult to distinguish the role of each channel separately (97). In bone, TRIC-B is the key player, where its role is to regulate the transmembrane flux of K^+ to maintain electroneutrality across the ER membrane in coordination with IP_3R channel mediated release of Ca^{2+} from the ER (93,95,96).

Patients and Mice

Type XIV OI is autosomal recessive form of OI caused by null mutations in *TMEM38B* (Table 1). A founder mutation in *TMEM38B* was first reported simultaneously in Bedouin families with OI in Israel and Saudi Arabia (98,99). Subsequent cases with different recessive defects in *TRIC-B* were reported in Albania, Pakistan, China, Egypt, Spain, and Turkey (85,100-103). Although these mutations are all null mutations, the extent of phenotypic variability among type XIV OI patients is striking, spanning from asymptomatic individuals to severe OI. Also, patients exhibit various combinations of clinical features such as *coxa vara*, fractures, and bowed long bones (101). Generally speaking, most patients with type XIV OI exhibit moderate OI severity, in the range of type IV OI, including osteoporosis, bowed limbs, wormian bones, and increased bone fragility (99). The onset of the first reported fracture among patients with the Bedouin founder mutation ranged from prenatal to 6 years of age (98). Distinct from other OI dominant and recessive types, the reduced BV/TV of type XIV OI is not associated with high bone turnover but rather with low bone resorption and reduced to normal numbers of osteoblasts (101). They also lack the bone hypermineralization found on qBEI in almost all OI types.

Fibroblasts and osteoblasts lacking TRIC-B exhibit impaired ER calcium influx kinetics. Since Ca^{+2} is a critical cofactor for multiple enzymes involved in procollagen assembly, folding, and modification, this leads to a global dysregulation of collagen synthesis. Posttranslational modification of collagen type I is uniquely altered in type XIV OI osteoblast and fibroblast cells, opposite to the overmodification of the collagen helix found in classical types II, III, and IV and recessive defects in procollagen prolyl 3-hydroxylation in types VII, VIII, and IX OI. In type XIV OI, collagen helical lysyl hydroxylation is reduced, due to LH1 dysfunction, despite attempted compensation though increased *PLOD1* transcription and increased LH1 protein levels (Fig. 4). There is a moderate increase in telopeptide lysine hydroxylation of patient procollagen that occurs due to increased lysyl hydroxylase 2 (LH2) levels, even though *PLOD2* transcripts and FKBP prolyl isomerase 65 protein are reduced. Notwithstanding the increased levels of protein disulfide isomerase (PDI) protein found in patient cells, disulfide catalysis by PDI, critical to the assembly of trimeric procollagen, is likely also compromised since procollagen assembly is delayed. Cyclophilin B protein (CyPB), a component of the procollagen proline 3-hydroxylation complex in the ER which also binds to both BiP and PDI, is decreased in *TMEM38B* null cells, resulting in modest reduction of collagen α1(I) P986 3-hydroxylation to levels seen in carriers of 3-hydroxylation defects (Fig. 4). CyPB is also the major collagen cis-trans isomerase and the peptidylprolyl isomerase (PPlase) for LH1, but collagen in TMEM38B null cells does not have delayed folding. A significant portion of the resulting misfolded procollagen is degraded intracellularly in TRIC-B null cells, causing reduced cellular collagen secretion (104).

Tric-b knockout mice die shortly after birth due to respiratory failure (93,95). The impaired IP_3R-mediated calcium release from the ER in alveolar epithelial cells results in intracellular store overload in these mice (95). Tric double knockout (*Tric-a/Tric-b*) mice suffer from cardiac dysfunction due to deformed cardiac myocytes with impaired intracellular calcium management; these mice are embryonic lethal (93). The *Tric-a* knockout mouse model was essential to the discovery that the Tric-b channel is able to function as a monovalent cation channel to deliver K^+ ions to the SR in response to loss of positive charge during acute phase of calcium release. (97). TRIC-B is vital for the ability of osteoblasts to deposit sufficient quantities of collagen in bone (105). *Tric-b* knockout mice display impaired bone mineralization and impaired ossification due to insufficiency of collagen deposited in ECM secondary to inhibition of collagen transport from ER to Golgi in osteoblasts (105). In patients, intracellular retention and degradation of procollagen similarly result in a marked decrease in collagen secretion by fibroblasts and osteoblasts (104).

Wnt Family Member 1 Defects—Type XV OI

Wnt/β-catenin signaling is one the major regulatory pathways in bone development. Human and murine studies showed that loss or gain of function of Wnt coreceptor low-density lipoprotein receptor-related protein 5 (LRP5) induced low or high bone mass phenotype, respectively, emphasizing the role of Wnt in bone formation (106-110) (Table 1). The Wnt/β-catenin pathway is activated by binding of Wnt ligand to the frizzled (Fz)/LRP5 or low-density lipoprotein receptor-related protein 6 (LRP6), which enhances β-catenin stability by inhibiting its phosphorylation by the degradation complex consisting of axin, adenomatous polyposis coli (APC), and glycogen synthase kinase 3 (GSK3). β-catenin then accumulates in the nucleus where it interacts with T cell factor/lymphoid enhancer-binding factor (TCF/LEF) and induces target gene expression (111) (Fig. 2).

In humans, mutations in Wnt family member 1 (WNT1) can cause either autosomal dominant or recessive type XV OI. Homozygous mutations in WNT1 were found to cause recessive OI, characterized by short stature, multiple vertebral compression fractures, kyphoscoliosis, and severe long bones fractures, with phenotypic severity ranging from moderate to progressive deforming (112-122). Intriguingly, heterozygous mutations in WNT1 cause dominantly inherited early-onset osteoporosis (113,115,123,124). Patients with recessive type XV OI have scleral hue ranging from white to bluish gray to blue. No dentinogenesis imperfecta was reported. Two features atypical for OI were also noted, in that the BMDD of patient bone was normal and bone histology showed low turnover. In either inheritance pattern, the mutated Wnt1 protein has reduced ability to activate the Wnt/β-catenin pathway, implicating its role in regulation of osteoblast function and bone homeostasis (113,115,124) (Fig. 2). Using crystal structure models, recessive p.Gly177Cys and dominant p.Arg235Trp substitutions in WNT1 were inferred to unfold Wnt1 segments important for binding to LRP5/6 or Fz receptors, respectively (113).

In the murine *Wnt1*$^{-/-}$ model, early postnatal lethality occurs due to disruption in midbrain and cerebellar development (125). In patients, *Wnt1* mutations have a more consistently skeletal impact, but emerging information points to a significant neurological component in type XV patients as well. About half of patients with *WNT1*-related OI have neurological or brain abnormalities, including dilated ventricles with cerebral atrophic changes, cerebellar hypoplasia with short midbrain, or type I Chiari malformation, and about 40% have severe intellectual disability or developmental delay (122). One striking feature has been the asymmetry of cerebellar hypoplasia seen in some patients, a rare feature among genetic types of cerebellar hypoplasia and one that raises the possibility of prenatal hemorrhage (126). Also, all patients with developmental delay or neurological defects exhibited bilateral ptosis, a unique finding that may facilitate the WNT1-OI diagnosis (122). Since some cases with central nervous system findings had consanguineous parents or an affected sibling without neurological defects, their neurological findings cannot be definitively attributed to the Wnt1 mutations, although the high percentage of affected children with a neurological abnormality makes mutation causality likely (114,115,120-122,126,127).

Further insight into mechanism of mutations in the Wnt1 pathway comes from the Swaying mouse (*Wnt1*$^{sw/sw}$), which carries a spontaneous single nucleotide deletion in *Wnt1* at the same site as reported in a patient, causing a frameshift and premature termination. *Wnt1*$^{sw/sw}$ mice survive postnatally; they have growth deficiency, spontaneous fractures, and osteopenic bone caused by a decrease in osteoblastic activity resulting in reduced collagen content in bone matrix. Their femora are weaker and break at lower ultimate load, but they are less brittle than WT, opposite to findings in classical and most recessive forms of OI. *Wnt1*$^{sw/sw}$ femora have reduced collagen mineralization, as evaluated by Raman spectroscopy, which is again atypical for OI (128). Both *Wnt1* null and *Wnt1*$^{sw/sw}$ mice show cerebellar defects; central impacts on bone fragility could also contribute to the skeletal phenotype (129).

Wnt1 expression has been traced to an osteocyte population in bone and to brain and femur in mouse (115). Murine models with cell-specific defects supported osteocytes as a source of WNT1, suggesting their role in regulation of bone formation was mediated through mammalian target of rapamycin complex 1 (mTORC1) signaling (130). Wnt1 signals from mesenchymal precursor cells were shown to act in juxtacrine manner and induce osteoblast differentiation and bone formation, while decreasing bone resorption (131).

Recently, mutations in *MESD*, a gene that encodes an endoplasmatic reticulum chaperone for the Wnt receptors LRP5 and LRP6, have been proposed to cause recessive OI (132) (Fig. 2, Table 1), although further data are needed to know whether these defects are better classified with OI or LRP5/6. Five independent individuals homozygous for truncation or frameshift mutations in the final exon of low-density lipoprotein receptor-related protein chaperone MESD (MESD) have a progressive deforming skeletal dysplasia, with recurrent fractures. Two individuals died in infancy of respiratory insufficiency. Bluish sclerae were present in the youngest patients. Older patients have oligodontia, a feature that could place these

patients with LRP6 loss-of-function mutations. Intellectual disability was present in 3 patients. Since the *MESD* mutations in patients are located downstream of the chaperone domain and upstream of the ER-retention domain in the protein, the investigators hypothesized that they are likely hypomorphic. Another recent paper reported compound heterozygous frameshift mutations in *MESD* exon 2 and exon 3 causing stillbirths (133). Three stillbirths presented with multiple intrauterine fractures and severe skeletal deformities. Histological analysis revealed uncoupled bone remodeling. Newly formed bone showed enlarged osteocytes and thickened canaliculi, with irregularly mineralized matrix. BMDD analysis indicated inhomogeneous, impaired mineralization of newly formed bone. The more severe phenotype may be related to the loss of the chaperone domain of *MESD* located in exon 2, leading to a complete protein loss of function and implying a role of *MESD* in early skeletal development.

Deletion of the *MESD* gene in mice causes embryonic lethality (134) and inhibits LRP5 and LRP6 trafficking (135). In patient fibroblasts, as well as cells transfected with *MESD* constructs, mutant *MESD* has the ability to chaperone and traffic LRP5, but is not retained in the ER. BP administration was not effective in these patients, likely related to low turnover status of bone. However, agents that enhance Wnt signaling such as antisclerostin antibody could potentially have therapeutic efficacy (132).

Types XVI and XVIII OI—Defects in RIP in Bone

Patients and Mice With OASIS Defects

Oasis (old astrocyte specifically induced-substance) is a transmembrane basic leucine zipper (bZIP) transcriptional factor that belongs to the CREB/ATF family, and was first identified by differential expression in long-term cultured murine astrocytes (136) (Table 1). When astrocytes are exposed to ER stressors such as thapsigargin or tunicamycin, OASIS is transported to the Golgi membrane and cleaved by the regulated intramembrane proteolysis (RIP) system, releasing the N-terminal cytoplasmic domain, which is then translocated into the nucleus to induce target gene transcription (137-139) (Fig. 4). Generation of *OASIS*$^{-/-}$ mice revealed the importance of this protein for bone formation (15). *OASIS*$^{-/-}$ mice have osteopenic bones, with decreased trabecular thickness (TbTh) underlying their decreased BV/TV. They are subject to spontaneous fractures and show growth retardation. Bone tissue, but not skin, has decreased type I collagen content, and decreased mineral density. This matrix insufficiency is based on the direct binding of OASIS to a UPR element-like sequence in the promoter of *Col1a1*, increasing collagen transcription. Oasis also promotes the secretion of bone matrix proteins, such as osteocalcin. Osteoblasts deficient in OASIS had enlarged ER with evident accumulation of procol(I)α1 and osteocalcin. When OASIS was overexpressed in osteoblast-like MC3T3-E1, exposure of the cells to ER stress led to cleavage of OASIS and its translocation into the nucleus, suggesting OASIS is activated by ER stress in osteoblasts. Stimulation of the same cells with bone morphogenetic protein 2 (BMP2), a bone formation regulator, induced mild/physiological ER stress and processing of OASIS was by RIP. This opens the testable concept that BMP regulation bone formation could involve induction of ER stress and activation of OASIS (15). Additionally, osteopenia and decreased expression of type I collagen, as well as expansion of enlarged ER, were rescued by osteoblast-specific overexpression of OASIS. Although growth retardation in *OASIS*$^{-/-}$ mice was not rescued by overexpression of OASIS, it was improved by treatment with growth hormone, implying *OASIS*$^{-/-}$ mice may have an impaired growth hormone/insulin-like growth factor 1 axis (140).

To date, defects in *CREB3L1*/OASIS have been reported in only 5 families or individuals with OI. A Turkish family had two severely affected children with *in utero* fractures of ribs and long bones and bowed limbs who were homozygous for deletion of the entire cAMP responsive element binding protein 3-like 1 (CREB3L1) gene. The first child lived 9 months without signs of immune deficiencies and died of cardiac insufficiency; the sibling was terminated *in utero*. No quantitative or structural defects of intracellular or secreted type I collagen were detected (141). Second, in a Lebanese family, an in-frame deletion of the codon for a single residue (p.Lys312del) caused a mild phenotype with blue sclerae and several childhood fractures in heterozygotes, while 3 homozygous infants had a severe lethal phenotype with marked rhizomelia, rib fractures and thin calvarium. The mutant OASIS was unable to bind to the UPR element-like sequence in the *COL1A1* promoter. Additionally, OASIS was shown to be important for expression of coat protein complex II (COPII) component Sec24 homolog D, involved in collagen protein trafficking (142). This impact of OASIS on the cellular collagen secretory machinery was also noted in cells from a terminated Turkish fetus with a homozygous missense mutation, associated with decreased transcription of Sec23 homolog A and Sec24 homolog D (143). Fourth, an 11-year old Somali boy had severe OI with blue sclerae, tooth agenesis, severe long bone fractures and lumbar spine DXA z-score = -6.1. He was homozygous for a PTC in OASIS. Marked decrease of type I collagen transcripts was noted in bone tissue, but not in skin, similar to findings in the *Oasis*$^{-/-}$ mouse (144). Most recently, the first adults with an OASIS defects were reported in an Indonesian pedigree. They have progressive

deforming OI of long bones and spine, but do not have blue sclerae or dentinogenesis imperfecta associated with their homozygous deletion, which is expected to produce a frameshift at p.Pro458. Cells were not available to determine the stability of the resulting *OASIS* transcript (145).

Patients With Defects in Site-2 Protease (Type XVIII OI) or Site-1 Protease

RIP signaling is an evolutionarily important process of cellular signal transduction, a mechanism which has been conserved from bacteria to humans. It has been implicated in processes of growth, differentiation, and ER stress response but is best known for its role in cholesterol metabolism (146,147). In addition to OASIS/CREB3L1, other substrates such as ATF6, one of the major transducers of UPR pathway (148), and sterol regulatory element-binding protein (SREBP), which regulates cholesterol metabolism (149), are processed by Class 2 RIP, a 2-stage cleavage reaction completed sequentially by site-1 and site-2 proteases (S1P and S2P, respectively). S1P is a serine protease with a single membrane-crossing helix and an active site with its catalytic triad (aspartate, histidine, serine) located in the lumen. S2P has multiple membranous domains and is a highly hydrophobic metalloprotease that contains an HEXXH zinc-binding motif important for its function (147) (Table 1). In response to retention of unfolded proteins in the ER, OASIS and other substrates are translocated from the ER membrane to the Golgi membrane, where they are sequentially cleaved by S1P and S2P. Their N-terminal fragment then translocates to the nucleus and regulates production of collagen and matrix components (138,139).

Type XVIII OI is also the first X-linked type. Moderately severe X-linked recessive OI was reported in 2 independent pedigrees from Thailand and Germany, caused by missense mutation in the *MBTPS2* gene that encodes S2P (150). The resulting substitutions are located in or near the S2P NPDG motif critical for S2P metal ion coordination. These patients have short stature, pre- and postnatal long bone and rib fractures, bowing, barrel chest, and vertebral compressions. Interestingly, substitutions elsewhere in S2P have been associated with cholesterol-related dermatological conditions ichthyosis follicularis, atrichia, and photophobia (IFAP); BRESEK/BRESHECK syndrome; and keratosis follicularis spinulosa decalvans (KFSD) (151-153). The OI patients do not share these symptoms; conversely, IFAP patients do not have a skeletal dysplasia. Affected OI fibroblasts and osteoblasts showed impaired, but not totally absent, cleavage of RIP substrates: OASIS, ATF6, and SREBP. Mass spectroscopy analysis of bone tissue collagen from 1 of the affected OI patients had less than half the normal level of hydroxylated lysine (K87), important for collagen cross-linking. This collagen finding is consistent with elevation of the urinary lysyl pyridinoline to hydroxylysyl pyridinoline ratio in 2 affected children. These data provide evidence that RIP is involved in regulation of bone homeostasis (150).

Interestingly, the sole patient associated with recessive mutations in the *MBTPS1* gene, encoding S1P, does not have OI, although the child does have features of a skeletal dysplasia. The patient shows growth retardation, kyphoscoliosis, and dysmorphic facial features, as well as elevated blood lysosomal enzymes. Chondrocytes in patient induced pluripotent stem cell teratomas displayed increased lysosomes and enlarged ER. S1P also proteolytically activates the cAMP responsive element binding protein 3-like 2 transcription factor (BBF2H7), which regulates expression of genes coding for proteins that form large collagen-secreting vesicles, such as *Tango1*. Impaired cleavage of BBF2H7 may be the cause of the collagen accumulation and increased apoptosis seen in patient cells. The patient also displayed elevated levels of urinary N-telopeptides, suggesting ECM degradation due to elevated levels of serum lysosomal enzymes might contribute to the skeletal phenotype (154).

S1P Deficient Mice

Cartilage-specific S1P knockout mice ($S1P^{cko}$) were generated before the patient with compound S1P mutations was reported. $S1P^{cko}$ mice develop severe chondrodysplasia and die shortly after birth, possibly due to respiratory distress caused by their small chest cavity. Bone histology shows lack of endochondral ossification. $S1P^{cko}$ bone sections show abnormal deposition of collagen fibrils and selective entrapment of type II collagen in chondrocytes. Electron microscopy of $S1P^{cko}$ tibia revealed enlarged ER, suggesting that S1P is important for ER stress induction by chondrocytes, necessary for cartilage synthesis, and plays an important role in bone development by regulating endochondral bone formation (155). When S1P was ablated by osterix promotor Cre-driven deletion, the mutant mice survived and developed an osteochondrodystrophy and variable scoliosis. Their bones have severe osteopenia with reduced mineral density, mineral apposition, and BFRs. S1P directly regulates skeletal development by regulating the pool of mesenchymal progenitors and osteoblastic differentiation (156).

Recently Proposed Candidate Gene for OI

Homozygous loss-of-function mutations in *CCDC134* have been recently identified as causative of a severe

recessive bone fragility syndrome in 3 Moroccan cases (157) (Table 1). *CCDC134* encodes a secretory protein responsible for inhibition of mitogen-activated protein kinase (MAPK) phosphorylation of extracellular signal-regulated kinase (ERK) or mitogen-activated protein kinase 8 (JNK) (158). Patients have short stature, multiple fractures, bowed long bones, pseudarthroses, and scleral hue ranging from white to grey, without dentinogenesis imperfecta. Histomorphometry yielded decreased Tb BV/TV but increased cortices, with normal MAR and BFR, an unusual pattern for OI. Increased Erk1/2 phosphorylation, decreased *COL1A1* and *OPN* expression, as well as decreased type I collagen were found in patient fibroblasts and osteoblasts, underlying reduced in vitro mineralization. Murine data supports a role for *Ccdc134* during embryonic development, perhaps functioning as a cytokine (159). KO mice were embryonically lethal and smaller than WT littermates. These reports suggest a role for *CCDC134* in bone formation through the MAPK/ERK signaling pathway, activating ERK1/2 phosphorylation and decreasing osteoblast differentiation as in neurofibromatosis 1 (160) and classic "dripping candle wax" melorheostosis (161). Further investigation of patient bone tissue will reveal whether coiled-coil domain-containing protein 134 (CCDC134) defects should be grouped with these conditions rather than recessive OI.

The latest gene discovered to be associated with OI is KDEL ER protein retention receptor 2 (*KDELR2*) (162) (Table 1, Fig. 1). Bi-allelic *KDELR2* variants were reported in 6 cases with multiple fractures beginning in childhood, long bone bowing, chest deformity, and short stature, given the diagnosis of progressive deforming OI (162).

KDELR2 encodes KDEL ER protein retention receptor 2, a member of the KDEL receptor family, localizes to the ER, Golgi complex, and intermediate ER-Golgi compartment (163). One KDELRs function is to facilitate the recovery of ER resident proteins from the acidic environment of the Golgi back to the neutral-pH ER using PH-dependent recognition by KDEL receptors of the c-terminus KDEL motif (Lys-Asp-Glu-Leu) (164). Among the proteins that contain the KDEL motif is the ER resident chaperone BiP (165).

Type I procollagen was reduced in media and cells of patient fibroblasts, as were intracellular levels of both FKPB65 and HSP47, which contain the KDEL motif (162). In addition, collagen fibrils were thin and imperfectly folded and an increase in HSP47 bound to monomeric and multimeric collagen molecules was revealed using electron microscopy. These defects in KDELR2, resulting in defective reverse transport, are a novel presumptive cause of recessive OI, given the known relationship of HSP47 to collagen function and regulation and the demonstrated defects in collagen in KDELR2 patients (162).

Material Properties and Mineralization of OI Bone

The increased fragility of OI bone is due to abnormalities in bone material properties as well as low bone mass (166). Both dominant and recessive OI-causing mutations affect bone tissue at multiple scales. The most notable changes involve the cross-links that give strength to bone and the mineralization that determines its brittleness (167,168).

Type I collagen, organized in heterotypic fibrils with types III and V collagen, comprises the major organic component of bone matrix. NCPs and proteoglycans interact with collagen at specific binding sites (169). Reduced collagen content of OI bone is associated with thin cortices and lower trabecular BV/TV on histomorphometry of both type I OI, caused by a quantitative defect in collagen without abnormality in the primary structure or posttranslational modification of type I collagen, and OI types II, III, and IV with defects in the primary structure of a collagen alpha chain and in posttranslational modification of the collagen triple helix (170). Both types of collagen defects are associated with increased osteoblasts and osteoclasts, supporting a high turnover bone metabolism. The proposed mechanism is that an increase in the microdamage occurring in bone matrix as a result of the impaired mechanical resistance may be the cause of the increase in remodeling. This also suggests that remodeling in OI patients is not effective since it is not improving the bone quality, but depositing new matrix that is still as impaired as the old matrix that was removed (171). The MAR, but not the mineralization lag time, was also reduced in both groups, pointing to a decreased osteoblast matrix production but a normal mineralization process (170).

On mechanical testing in femora of murine models, OI bone (types I-IV, VI, VII, VIII, IX, XIII) is generally less stiff, has a lower yield point (the deformation at which bone cannot resume its prebending configuration), fractures at a lower ultimate load, and is more brittle (reduced postyield displacement) than normal bone (78,172,173). Correlating these whole bone defects in strength with particular molecular defects is difficult. Complex factors such as increased bone microcracks and altered collagen cross-link patterns have adverse effects on bone strength. Cross-links between collagen monomers are formed by lysyl oxidase and lysyl hydroxylase. Trivalent collagen cross-links measured as biomarkers result from collagen resorption (174). In the *oim/oim* mouse, the decrease in enzymatic collagen cross-links and 30% increase in nonenzymatic collagen cross-links, also called advance glycation end products, contribute to decreased bone toughness, resulting in minimal resistance to microcrack propagation (175).

Hypermineralization of bone tissue is a cardinal unifying feature of almost all OI types. This is the major tissue property underlying OI bone brittleness, which refers to its susceptibility to fracture by snapping when bent or displaced beyond the yield point. This discovery of OI bone hypermineralization, first made by Boyde et al (176) in 1999, came as a surprise because DXA bone density is almost always decreased in OI. The source of this apparent paradox lies in the imaging technique; DXA is a 2D-imaging modality that relies on comparison of patient bone with a phantom and is dependent on both mineral quantity and organization, while BMDD can be determined directly on bone sections using qBEI. BMDD allows direct determination of different parameters such as mean calcium concentration (CaMean), obtained from integrated area under BMDD curve; peak calcium content (CaPeak), is the most frequently measured calcium concentration; the width of calcium content distribution (CaWidth), which reflects variation in mineralization density; the highly mineralized area of bone (CaHigh), which is measured as the percentage of mineralized bone area above the 95th percentile; and the area of bone with low amounts of mineralized bone (CaLow), which is measured as the percentage of mineralized bone area below the 5th percentile (177). Patients with either qualitative or haploinsufficiency mutations in type I collagen show a similar increase in mean and peak calcium content of bone on BMDD (166). Similarly, the mineral particle width, determined with combined small-angle X-ray scattering (SAXS), which provides data on mineral crystal orientation and shape in bone, and wide-angle X-ray diffraction (WAXD), which characterizes structural parameters of hydroxy appetite crystals (178), has an equivalent increase in the packing density of normal width crystals in bone with collagen structural or haploinsufficiency defects. This similarity of mineralization quantity and organization between OI types is counterintuitive, in that it does not correlate with either the severity of OI phenotype or the procollagen structural changes. Factors other than the collagen itself have been proposed as responsible for the hypermineralization of OI bone (179,180), and this proposal is supported by the occurrence of bone hypermineralization in recessive forms without primary defects in collagen structure (167,168,181). Interestingly, processing of the procollagen C-propeptide also affects bone mineralization. Mutations in the procollagen C-proteinase cleavage site (28) lead to OI with uniformly moderate severity. Bone hypermineralization on BMDD (28) is shifted further to the right of the collagen-based OI curve, with calcium levels higher than any other forms of OI. Histomorphometry showed increased trabecular volume and cortical thickness with hyperosteoidosis (29), as well as normal to elevated L1-L2 DXA values. Correspondingly, recessive mutations in the C-proteinase, BMP1, have a similar outcome to the dominant mutations in the cleavage site and cause type XIII OI, with hyperosteoidosis and hypermineralization on BMDD similar to cleavage site defects in most cases (182).

Bone hypermineralization is also evident in types VII and VIII OI, which have recessive defects in the components of the procollagen prolyl 3-hydroxylation complex. These patients have normal collagen primary structure and absence/reduction of α1(I)Pro986 3-hydroxylation. They also have full overmodification of collagen helical lysines (183-185). Both type VII patients and Crtap$^{-/-}$ mice have hypermineralization of bone, with notable increase of highly mineralized area of bone (167,183). In patients with type VIII OI caused by recessive defects in P3H1, the enzymatic component of the complex, mean and peak mineralization were indistinguishable from type VII, but amount of CaLow area was increased in both cortical and cancellous bone in conjunction with a patchy increase in osteoid (181).

Patients with types V and VI OI have normal collagen primary structure and posttranslational modification yet share the characteristic OI hypermineralization. Both cortical and cancellous bone material from type V OI, caused by a gain-of-function mutation in the transmembrane protein BRIL, is hypermineralized. In addition, osteocyte lacunar size and density were increased in type V OI bone compared to age-matched controls (71). In type VI OI bone, Fratzl-Zelman et al reported areas of hypermineralization exceeding that found in collagen-based OI bone, which coexist with areas of abnormally low mineralization, as well as a smaller mineral particle size than in collagen-based OI bone (168). Interestingly, types V and VI OI each have other abnormalities of mineralization. Type V OI is characterized by active mineralization of the interosseous membrane of the forearm and a dense metaphyseal band, while type VI OI bone has prolonged mineral lag time and broad osteoid seams (66,77).

The issue of bone hypermineralization is still unsettled for the OI types in which RIP is impaired. Bone tissue was not available for BMDD on the first patients reported with missense mutations in MBTPS2 (type XVIII OI) (150). A child with recessive OASIS deficiency due to a premature stop codon in *CREB3L1* was reported to have increased mineralization by BMDD; however, this child had been treated with BP since age 3 months, so it is not possible to draw a clear conclusion from a biopsy obtained at age 11 years (144).

Types XIV and XV OI, caused by mutations in *TMEM38B* and *WNT1*, respectively, are exceptions to the general rule that OI bone is hypermineralized. BMDD of types XIV and XV OI patient bone is normal (101,186).

Osteoblasts cultured from *Tric-b* knockout mice deposit less mineral and collagen in vitro (105). Bone from type XV patients with *WNT1* defects showed low turnover, in contrast to the high turnover found in most OI types (123). MC3T3 cells stably expressing WNT^{C218G} and $WNT^{S295,*}$ mutations deposit less mineral in culture (115). The swaying mouse model ($Wnt1^{sw/sw}$) exhibits reduced bone strength associated with lower bone mineral and collagen content by Raman spectroscopy (128).

Treatment Approaches to OI

Nonpharmacological

The broad clinical range of OI between and within OI types prevents a one-size-fits-all strategy to clinical management. Nonetheless, common features lead to a general approach to patients who have symptoms including bone fragility, muscle weakness, the secondary features of OI and quality-of-life (QOL) issues. A multidisciplinary team is the best approach for integration of these issues.

Physical rehabilitation and therapy are a mainstay of OI management from the time of diagnosis and throughout adult life (187). Acute issues such as recovery of ambulatory or upper limb function after a fracture should be dealt with expeditiously. However, self-care functions and QOL require ongoing periodic intervention to maintain joint range of motion and use of ambulatory aids and optimum mobility devices. A special focus of physical therapy across the OI types is muscle weakness (188). Careful periodic evaluation of the strength of individual muscle groups and targeted at-home and professional physical therapy are critical to obtaining and maintaining independent living. Physical rehabilitation is also a useful adjunct to pharmacological therapy. The range of activities in which individuals with different types of OI can safely engage is best determined in consultation with a physiatrist with experience treating OI patients.

Orthopedic management of OI encompasses lower and upper extremity, as well as spine surgery. For patients with ambulation potential, corrective surgery followed by physical therapy should be undertaken as the child becomes otherwise ready to walk. This generally involves cutting or breaking of long bones to allow realignment and insertion of an intramedullary rod to provide stabilization and some strength. While an open osteotomy may be required depending on the extent of long bone deformity, the percutaneous procedures involving the Fassier-Duval elongating rod have now become the approach of choice for both lower and upper extremities (189,190). The elongating rods allow a greater interval between surgeries *vs* straight rods but have an equivalent complication rate of rod migration. Rod diameter should be chosen to provide sufficient support for the particular bone but should not represent the maximum diameter that can be reamed into the medullary cavity, as this will result in diaphyseal atrophy from weight unloading. Prolonged postoperative immobilization should be avoided. The use of plates and screw should be avoided if at all possible for cases more severe than type I OI. Experience has shown that the junction of the plated and nonplated bone is at high risk for fractures and the plated portion does not fill in around screws or residual screw holes resulting in a nonfunctional bone material looking like Swiss-cheese. Scoliosis in OI does not respond to external bracing, such as the Milwaukee brace, and surgery should be undertaken before a 60-degree curve is attained. Spinal fusion with Harrington rod placement can provide stabilization but will not fully correct the curve. Newer approaches utilize pedicle screw fixation systems with biomechanical advantages but long-term effectiveness is not yet known (191,192). As the OI population ages, osteoarthritis is an emerging issue. Hip and knee arthroplasties are most successful in this population with custom implants based on computer-assisted design (193).

The secondary features of OI vary among the OI types. Dentinogenesis imperfecta (DI) breeds true in OI pedigrees. Dentinogenesis imperfecta may manifest as a greyish translucency of the dentin layer or as yellow-brown teeth with a propensity to crumble. Dental manifestations (194) are more severe in childhood than with permanent teeth; hence, early attention to teeth with an OI-experienced professional is warranted to prevent cavities and provide appropriate restoration. Pulmonary complications are the leading cause of morbidity and mortality in OI (195). Scoliosis over 60 degrees contributes to the pulmonary deficiency of OI patients, associated with development of obstructive pulmonary disease (196). It is also becoming clear that there is an intrinsic component to the pulmonary disease of OI, likely based on the presence of type I collagen in lung parenchyma. Children with types III and IV OI in a longitudinal natural history study have been shown to have decreasing pulmonary function throughout childhood, even in the group without scoliosis, while the rate of decline is greater in those who also have scoliosis (61). Parenchymal lung defects have also been reported in the Aga2 mouse, with a collagen defect, and in the CRTAP KO mouse, suggesting this may be an issue for recessive types of OI as well (61,197). The most commonly reported cardiac defects are aortic root dilatation and left-sided valvular regurgitation; aortic dissection occurs rarely (198). Patients should have echocardiography periodically starting in childhood to detect these features early. Similarly, hearing loss is a relatively common secondary feature of OI with

functional manifestation between the second to fourth decades of life (199,200). However, about 5% of patients develop hearing loss requiring hearing aids or even cochlear implants during childhood and periodic audiology should begin during the school years (201). Likewise, skull base abnormalities, including platybasia, basilar invagination (BI) or basilar impression can have serious consequences and monitoring should begin in childhood (202,203). Patients with height z-score < –3 may be particularly at risk. Occurrence of BI is not prevented by BP treatment (204).

QOL of individuals with OI is an increasing subject of focus. Decreased physical functioning and environmental barriers can impede independence and life satisfaction. Young adults with OI increasingly take advantage of opportunities for college education, independent living, and careers. The impact of pharmacological therapy on OI QOL is unclear.

Pharmacological Approaches

BPs such as alendronate, pamidronate (most commonly), and zolendronic acid are widely administered to treat OI types with collagen defects and some recessive forms (205,206). These antiresorptive drugs act to inhibit bone resorption by osteoclasts; they are directly deposited on the bone surface where their endocytosis by osteoclasts induces apoptosis. Although the mutant collagen would still be deposited in bone matrix, inhibiting bone resorption will result in an overall increase in bone mass. Conversely, prolonged treatment may alter the material properties of bone, potentially causing cellular adynamic bone, with increased potential for microcrack propagation into fractures.

Disagreement has continued about the effects of long-term usage of BP focusing on benefits *vs* detrimental effects, dosing, and duration of treatment. Most children with OI who were treated with BP have experienced increased areal bone density z-score of about 1.5 SD in the first year and relief of vertebral compressions (207,208). In addition, bone microarchitecture is improved. However, controlled trials are equivocal about fracture reduction. Two Cochran reports and a separate meta-analysis (209-211) did not support a statistical improvement in fracture occurrence. Although these analyses have been challenged by supporters of BP treatment, the effect on fractures in pediatric OI is not as robust as originally hoped. Cochran report analyses also did not support improved pain or mobility status of treated patients. Another expected outcome of BP treatment was that relief of vertebral compressions would decrease the scoliosis of OI, which would, in turn, limit serious secondary pulmonary defects due to thoracic deformity. Unfortunately, careful analyses revealed that the incidence and extent of scoliosis was unchanged with BP treatment, although a modest delay in curve development may occur in progressive deforming OI (212). Anecdotal reports of fractures at the junction of BP-treated/untreated bone have been the basis of a proposal to treat children until epiphyseal closure (213); similar fractures have not been seen in children who have received lower cumulative doses of BP.

Bone-building, rather than antiresorptive, drugs hold some promise for modifying the fragility of OI bone without increasing brittleness. Antibodies to sclerostin, a negative regulator of bone formation in the Wnt pathway, have been approved for treatment of postmenopausal osteoporosis. These antibodies have been tested in various OI murine models (214-217) and have shown improved bone stiffness and strength. Bone brittleness was not further impaired and Raman spectroscopy suggested that elevated bone mineralization might be improved in newly formed bone during treatment. Another antibody therapy, anti-TGFβ antibody improved trabecular and cortical bone mass and strength in $Crtap^{-/-}$ mice, as well as lung ultrastructure (218). A safety trial with this antibody is underway in the OI Brittle Bone Consortium. Both antibody therapies are relatively short-acting, and bone gain would require a small dose of BP to solidify gains after treatment (219,220).

Gene and Cell Therapy

The most promising future treatment prospects of OI caused by defective collagen structure seek to emulate the 2 mechanisms by which mutations are mitigated in nature—namely, silencing a mutant allele and cellular mosaicism. Various gene-silencing techniques (ribozymes, small interfering RNA, and short hairpin RNA) have been investigated in vitro, to copy the situation in type I OI in which the mutant allele is silent (221). This approach would result in a milder OI, rather than cure the condition. Although these approaches can result in near complete silencing in the test tube, the silencing is generally not complete in cells, and the duration of the effect is limited.

Cell transplantation mimics the situation in mosaic parents of OI children, who have 2 populations of cells (mutant and nonmutant) and rarely come to clinical attention prior to the birth of their child. The challenge for this approach has been uptake of cells into bone. Studies in murine models using stem cells reported improved bone mechanics despite cell uptake less than a few percentage points (222,223). More recently (224) higher levels of cell transplantation have been attained with local transplantation, and cells tagged with green fluorescent protein (GFP)

have been retransplanted to a secondary recipient, supporting their viability. A clinical trial currently underway in Europe is transplanting fetal mesenchymal stem cells during the first months after birth or in utero.

Acknowledgments

Financial Support: The writing of this review was supported by intramural funding from the Eunice Kennedy Shriver National Institute of Child Health and Human Development (NICHD, NIH) IRP to JCM, ZIA HD008830-15 and ZIA HD000408-38.

Additional Information

Correspondence: Joan C Marini, Chief, Section on Heritable Disorders of Bone and Extracellular Matrix, NICHD, NIH, Bldg, 49; Rm 5A52, 49 Convent Drive, Bethesda, MD 20892, USA. Email: oidoc@helix.nih.gov.

Disclosures: No conflict of interest for all authors.

Data Availability: All data generated or analyzed during this study are included in this published article or in the data repositories listed in references.

References

1. Gatti D, Rossini M, Viapiana O, et al. Teriparatide treatment in adult patients with osteogenesis imperfecta type I. *Calcif Tissue Int*. 2013;**93**(5):448-452.
2. Orwoll ES, Shapiro J, Veith S, et al. Evaluation of teriparatide treatment in adults with osteogenesis imperfecta. *J Clin Invest*. 2014;**124**(2):491-498.
3. Nicol L, Srikanth P, Henriksen K, et al. Widespread disturbance in extracellular matrix collagen biomarker responses to teriparatide therapy in osteogenesis imperfecta. *Bone*. 2021;**142**:115703.
4. Forlino A, Marini JC. Osteogenesis imperfecta. *Lancet*. 2016;**387**(10028):1657-1671.
5. Kuivaniemi H, Tromp G, Prockop DJ. Mutations in collagen genes: causes of rare and some common diseases in humans. *Faseb J*. 1991;**5**(7):2052-2060.
6. Lehmann HW, Rimek D, Bodo M, et al. Hydroxylation of collagen type I: evidence that both lysyl and prolyl residues are overhydroxylated in osteogenesis imperfecta. *Eur J Clin Invest*. 1995;**25**(5):306-310.
7. Cabral WA, Fratzl-Zelman N, Weis M, et al. Substitution of murine type I collagen A1 3-hydroxylation site alters matrix structure but does not recapitulate osteogenesis imperfecta bone dysplasia. *Matrix Biol*. 2020;**90**:20-39.
8. Yamauchi M, Sricholpech M. Lysine post-translational modifications of collagen. *Essays Biochem*. 2012;**52**:113-133.
9. Forlino A, Porter FD, Lee EJ, Westphal H, Marini JC. Use of the Cre/lox recombination system to develop a non-lethal knock-in murine model for osteogenesis imperfecta with an alpha1(I) G349C substitution. Variability in phenotype in BrtlIV mice. *J Biol Chem*. 1999;**274**(53):37923-37931.
10. Reich A, Cabral W, Marini J. Homogeneous mutant collagen in osteogenesis imperfecta model mice leads to improved bone phenotype through multiple pathways [Abstract P38]. Program of the American Society for Bone and Mineral Research Topical Meeting on Bone and Skeletal Muscle Interactions, Kansas City, MO, 2012.
11. Forlino A, Kuznetsova NV, Marini JC, Leikin S. Selective retention and degradation of molecules with a single mutant alpha1(I) chain in the Brtl IV mouse model of OI. *Matrix Biol*. 2007;**26**(8):604-614.
12. Bianchi L, Gagliardi A, Gioia R, et al. Differential response to intracellular stress in the skin from osteogenesis imperfecta Brtl mice with lethal and non lethal phenotype: a proteomic approach. *J Proteomics*. 2012;**75**(15):4717-4733.
13. Forlino A, Tani C, Rossi A, et al. Differential expression of both extracellular and intracellular proteins is involved in the lethal or nonlethal phenotypic variation of BrtlIV, a murine model for osteogenesis imperfecta. *Proteomics*. 2007;**7**(11):1877-1891.
14. Bianchi L, Gagliardi A, Maruelli S, et al. Altered cytoskeletal organization characterized lethal but not surviving Brtl+/– mice: insight on phenotypic variability in osteogenesis imperfecta. *Hum Mol Genet*. 2015;**24**(21):6118-6133.
15. Murakami T, Saito A, Hino S, et al. Signalling mediated by the endoplasmic reticulum stress transducer OASIS is involved in bone formation. *Nat Cell Biol*. 2009;**11**(10):1205-1211.
16. Besio R, Iula G, Garibaldi N, et al. 4-PBA ameliorates cellular homeostasis in fibroblasts from osteogenesis imperfecta patients by enhancing autophagy and stimulating protein secretion. *Biochim Biophys Acta Mol Basis Dis*. 2018;**1864**(5 Pt A):1642-1652.
17. Mirigian LS, Makareeva E, Mertz EL, et al. Osteoblast malfunction caused by cell stress response to procollagen misfolding in α2 (I)-G610C mouse model of osteogenesis imperfecta. *J Bone Miner Res*. 2016;**31**(8):1608-1616.
18. Omari S, Makareeva E, Roberts-Pilgrim A, et al. Noncanonical autophagy at ER exit sites regulates procollagen turnover. *Proc Natl Acad Sci U S A*. 2018;**115**(43):E10099-E10108.
19. Scheiber AL, Guess AJ, Kaito T, et al. Endoplasmic reticulum stress is induced in growth plate hypertrophic chondrocytes in G610C mouse model of osteogenesis imperfecta. *Biochem Biophys Res Commun*. 2019;**509**(1):235-240.
20. Bateman JF, Sampurno L, Maurizi A, et al. Effect of rapamycin on bone mass and strength in the α2(I)-G610C mouse model of osteogenesis imperfecta. *J Cell Mol Med*. 2019;**23**(3):1735-1745.
21. Jeong Y, Carleton SM, Gentry BA, et al. Hindlimb skeletal muscle function and skeletal quality and strength in+/G610C mice with and without weight-bearing exercise. *J Bone Miner Res*. 2015;**30**(10):1874-1886.
22. Daley E, Streeten EA, Sorkin JD, et al. Variable bone fragility associated with an Amish COL1A2 variant and a knock-in mouse model. *J Bone Miner Res*. 2010;**25**(2):247-261.
23. Gistelinck C, Gioia R, Gagliardi A, et al. Zebrafish collagen type I: molecular and biochemical characterization of the major structural protein in bone and skin. *Sci Rep*. 2016;**6**:21540.
24. Fisher S, Jagadeeswaran P, Halpern ME. Radiographic analysis of zebrafish skeletal defects. *Dev Biol*. 2003;**264**(1):64-76.
25. Gioia R, Tonelli F, Ceppi I, et al. The chaperone activity of 4PBA ameliorates the skeletal phenotype of Chihuahua, a zebrafish

model for dominant osteogenesis imperfecta. *Hum Mol Genet*. 2017;**26**(15):2897-2911.
26. Fiedler IAK, Schmidt FN, Wölfel EM, et al. Severely impaired bone material quality in chihuahua zebrafish resembles classical dominant human osteogenesis imperfecta. *J Bone Miner Res*. 2018;**33**(8):1489-1499.
27. Gistelinck C, Kwon RY, Malfait F, et al. Zebrafish type I collagen mutants faithfully recapitulate human type I collagenopathies. *Proc Natl Acad Sci U S A*. 2018;**115**(34):E8037-E8046.
28. Lindahl K, Barnes AM, Fratzl-Zelman N, et al. COL1 C-propeptide cleavage site mutations cause high bone mass osteogenesis imperfecta. *Hum Mutat*. 2011;**32**(6):598-609.
29. Cundy T, Dray M, Delahunt J, et al. Mutations that alter the carboxy-terminal-propeptide cleavage site of the chains of Type I procollagen are associated with a unique osteogenesis imperfecta phenotype. *J Bone Miner Res*. 2018;**33**(7):1260-1271.
30. Wozney JM, Rosen V, Celeste AJ, et al. Novel regulators of bone formation: molecular clones and activities. *Science*. 1988;**242**(4885):1528-1534.
31. Kessler E, Takahara K, Biniaminov L, Brusel M, Greenspan DS. Bone morphogenetic protein-1: the type I procollagen C-proteinase. *Science*. 1996;**271**(5247):360-362.
32. Li SW, Sieron AL, Fertala A, Hojima Y, Arnold WV, Prockop DJ. The C-proteinase that processes procollagens to fibrillar collagens is identical to the protein previously identified as bone morphogenic protein-1. *Proc Natl Acad Sci U S A*. 1996;**93**(10):5127-5130.
33. Scott IC, Blitz IL, Pappano WN, et al. Mammalian BMP-1/Tolloid-related metalloproteinases, including novel family member mammalian Tolloid-like 2, have differential enzymatic activities and distributions of expression relevant to patterning and skeletogenesis. *Dev Biol*. 1999;**213**(2):283-300.
34. von Marschall Z, Fisher LW. Decorin is processed by three isoforms of bone morphogenetic protein-1 (BMP1). *Biochem Biophys Res Commun*. 2010;**391**(3):1374-1378.
35. Scott IC, Imamura Y, Pappano WN, et al. Bone morphogenetic protein-1 processes probiglycan. *J Biol Chem*. 2000;**275**(39):30504-30511.
36. Ge G, Seo NS, Liang X, Hopkins DR, Höök M, Greenspan DS. Bone morphogenetic protein-1/tolloid-related metalloproteinases process osteoglycin and enhance its ability to regulate collagen fibrillogenesis. *J Biol Chem*. 2004;**279**(40):41626-41633.
37. Uzel MI, Scott IC, Babakhanlou-Chase H, et al. Multiple bone morphogenetic protein 1-related mammalian metalloproteinases process pro-lysyl oxidase at the correct physiological site and control lysyl oxidase activation in mouse embryo fibroblast cultures. *J Biol Chem*. 2001;**276**(25):22537-22543.
38. Steiglitz BM, Ayala M, Narayanan K, George A, Greenspan DS. Bone morphogenetic protein-1/Tolloid-like proteinases process dentin matrix protein-1. *J Biol Chem*. 2004;**279**(2):980-986.
39. Ge G, Greenspan DS. BMP1 controls TGFbeta1 activation via cleavage of latent TGFbeta-binding protein. *J Cell Biol*. 2006;**175**(1):111-120.
40. Suzuki N, Labosky PA, Furuta Y, et al. Failure of ventral body wall closure in mouse embryos lacking a procollagen C-proteinase encoded by Bmp1, a mammalian gene related to Drosophila tolloid. *Development*. 1996;**122**(11):3587-3595.
41. Clark TG, Conway SJ, Scott IC, et al. The mammalian Tolloid-like 1 gene, Tll1, is necessary for normal septation and positioning of the heart. *Development*. 1999;**126**(12):2631-2642.
42. Muir AM, Ren Y, Butz DH, et al. Induced ablation of Bmp1 and Tll1 produces osteogenesis imperfecta in mice. *Hum Mol Genet*. 2014;**23**(12):3085-3101.
43. Martínez-Glez V, Valencia M, Caparrós-Martín JA, et al. Identification of a mutation causing deficient BMP1/mTLD proteolytic activity in autosomal recessive osteogenesis imperfecta. *Hum Mutat*. 2012;**33**(2):343-350.
44. Valencia M, Caparrós-Martin JA, Sirerol-Piquer MS, et al. Report of a newly indentified patient with mutations in BMP1 and underlying pathogenetic aspects. *Am J Med Genet A*. 2014;**164A**(5):1143-1150.
45. Pollitt RC, Saraff V, Dalton A, et al. Phenotypic variability in patients with osteogenesis imperfecta caused by BMP1 mutations. *Am J Med Genet A*. 2016;**170**(12):3150-3156.
46. Syx D, Guillemyn B, Symoens S, et al. Defective proteolytic processing of fibrillar procollagens and prodecorin due to biallelic BMP1 mutations results in a severe, progressive form of osteogenesis imperfecta. *J Bone Miner Res*. 2015;**30**(8):1445-1456.
47. Kuchta K, Knizewski L, Wyrwicz LS, Rychlewski L, Ginalski K. Comprehensive classification of nucleotidyltransferase fold proteins: identification of novel families and their representatives in human. *Nucleic Acids Res*. 2009;**37**(22):7701-7714.
48. Watanabe T, Yamamoto T, Tsukano K, Hirano S, Horikawa A, Michiue T. Fam46a regulates BMP-dependent pre-placodal ectoderm differentiation in Xenopus. *Development*. 2018;**145**(20).
49. Diener S, Bayer S, Sabrautzki S, et al. Exome sequencing identifies a nonsense mutation in Fam46a associated with bone abnormalities in a new mouse model for skeletal dysplasia. *Mamm Genome*. 2016;**27**(3-4):111-121.
50. Doyard M, Bacrot S, Huber C, et al. FAM46A mutations are responsible for autosomal recessive osteogenesis imperfecta. *J Med Genet*. 2018;**55**(4):278-284.
51. Barragán I, Borrego S, Abd El-Aziz MM, et al. Genetic analysis of FAM46A in Spanish families with autosomal recessive retinitis pigmentosa: characterisation of novel VNTRs. *Ann Hum Genet*. 2008;**72**(Pt 1):26-34.
52. Symoens S, Hulmes DJ, Bourhis JM, Coucke PJ, De Paepe A, Malfait F. Type I procollagen C-propeptide defects: study of genotype-phenotype correlation and predictive role of crystal structure. *Hum Mutat*. 2014;**35**(11):1330-1341.
53. Bourhis JM, Mariano N, Zhao Y, et al. Structural basis of fibrillar collagen trimerization and related genetic disorders. *Nat Struct Mol Biol*. 2012;**19**(10):1031-1036.
54. Barnes AM, Ashok A, Makareeva EN, et al. COL1A1 C-propeptide mutations cause ER mislocalization of procollagen and impair C-terminal procollagen processing. *Biochim Biophys Acta Mol Basis Dis*. 2019;**1865**(9):2210-2223.
55. Pace JM, Kuslich CD, Willing MC, Byers PH. Disruption of one intra-chain disulphide bond in the carboxyl-terminal propeptide of the proalpha1(I) chain of type I procollagen permits slow assembly and secretion of overmodified, but stable procollagen trimers and results in mild osteogenesis imperfecta. *J Med Genet*. 2001;**38**(7):443-449.

56. Doan N-D, Hosseini AS, Bikovtseva AA, et al. Elucidation of proteostasis defects caused by osteogenesis imperfecta mutations in the collagen-α2 (I) C-propeptide domain. *J Biol Chem*. 2020;**295**(29):9959-9973.
57. Chessler SD, Byers PH. BiP binds type I procollagen pro alpha chains with mutations in the carboxyl-terminal propeptide synthesized by cells from patients with osteogenesis imperfecta. *J Biol Chem*. 1993;**268**(24):18226-18233.
58. Lamandé SR, Chessler SD, Golub SB, et al. Endoplasmic reticulum-mediated quality control of type I collagen production by cells from osteogenesis imperfecta patients with mutations in the proα1 (I) chain carboxyl-terminal propeptide which impair subunit assembly. *J Biol Chemi*. 1995;**270**(15):8642-8649.
59. Fitzgerald J, Lamandé SR, Bateman JF. Proteasomal degradation of unassembled mutant type I collagen pro-α1 (I) chains. *J Biol Chem*. 1999;**274**(39):27392-27398.
60. Lisse TS, Thiele F, Fuchs H, et al. ER stress-mediated apoptosis in a new mouse model of osteogenesis imperfecta. *PLoS Genet*. 2008;**4**(2):e7.
61. Thiele F, Cohrs CM, Flor A, et al. Cardiopulmonary dysfunction in the Osteogenesis imperfecta mouse model Aga2 and human patients are caused by bone-independent mechanisms. *Hum Mol Genet*. 2012;**21**(16):3535-3545.
62. Semler O, Garbes L, Keupp K, et al. A mutation in the 5'-UTR of IFITM5 creates an in-frame start codon and causes autosomal-dominant osteogenesis imperfecta type V with hyperplastic callus. *Am J Hum Genet*. 2012;**91**(2):349-357.
63. Cho TJ, Lee KE, Lee SK, et al. A single recurrent mutation in the 5'-UTR of IFITM5 causes osteogenesis imperfecta type V. *Am J Hum Genet*. 2012;**91**(2):343-348.
64. Hanagata N. IFITM5 mutations and osteogenesis imperfecta. *J Bone Miner Metab*. 2016;**34**(2):123-131.
65. Hanagata N, Li X, Morita H, Takemura T, Li J, Minowa T. Characterization of the osteoblast-specific transmembrane protein IFITM5 and analysis of IFITM5-deficient mice. *J Bone Miner Metab*. 2011;**29**(3):279-290.
66. Glorieux FH, Rauch F, Plotkin H, et al. Type V osteogenesis imperfecta: a new form of brittle bone disease. *J Bone Miner Res*. 2000;**15**(9):1650-1658.
67. Rauch F, Moffatt P, Cheung M, et al. Osteogenesis imperfecta type V: marked phenotypic variability despite the presence of the IFITM5 c.-14C>T mutation in all patients. *J Med Genet*. 2013;**50**(1):21-24.
68. Patoine A, Gaumond MH, Jaiswal PK, Fassier F, Rauch F, Moffatt P. Topological mapping of BRIL reveals a type II orientation and effects of osteogenesis imperfecta mutations on its cellular destination. *J Bone Miner Res*. 2014;**29**(9):2004-2016.
69. Reich A, Bae AS, Barnes AM, et al. Type V OI primary osteoblasts display increased mineralization despite decreased COL1A1 expression. *J Clin Endocrinol Metab*. 2015;**100**(2):E325-E332.
70. Shapiro JR, Lietman C, Grover M, et al. Phenotypic variability of osteogenesis imperfecta type V caused by an IFITM5 mutation. *J Bone Miner Res*. 2013;**28**(7):1523-1530.
71. Blouin S, Fratzl-Zelman N, Glorieux FH, et al. Hypermineralization and high osteocyte lacunar density in osteogenesis imperfecta Type V bone indicate exuberant primary bone formation. *J Bone Miner Res*. 2017;**32**(9):1884-1892.
72. Rauch F, Geng Y, Lamplugh L, et al. Crispr-Cas9 engineered osteogenesis imperfecta type V leads to severe skeletal deformities and perinatal lethality in mice. *Bone*. 2018;**107**:131-142.
73. Sekiya A, Okano-Kosugi H, Yamazaki CM, Koide T. Pigment epithelium-derived factor (PEDF) shares binding sites in collagen with heparin/heparan sulfate proteoglycans. *J Biol Chem*. 2011;**286**(30):26364-26374.
74. Li F, Cain JD, Tombran-Tink J, Niyibizi C. Pigment epithelium-derived factor (PEDF) reduced expression and synthesis of SOST/sclerostin in bone explant cultures: implication of PEDF-osteocyte gene regulation in vivo. *J Bone Miner Metab*. 2019;**37**(5):773-779.
75. Gattu AK, Swenson ES, Iwakiri Y, et al. Determination of mesenchymal stem cell fate by pigment epithelium-derived factor (PEDF) results in increased adiposity and reduced bone mineral content. *Faseb J*. 2013;**27**(11):4384-4394.
76. Huang KT, Hsu LW, Chen KD, Kung CP, Goto S, Chen CL. Decreased PEDF Expression promotes adipogenic differentiation through the up-regulation of CD36. *Int J Mol Sci*. 2018;**19**(12).
77. Glorieux FH, Ward LM, Rauch F, Lalic L, Roughley PJ, Travers R. Osteogenesis imperfecta type VI: a form of brittle bone disease with a mineralization defect. *J Bone Miner Res*. 2002;**17**(1):30-38.
78. Bogan R, Riddle RC, Li Z, et al. A mouse model for human osteogenesis imperfecta type VI. *J Bone Miner Res*. 2013;**28**(7):1531-1536.
79. Rajagopal A, Homan EP, Joeng KS, et al. Restoration of the serum level of SERPINF1 does not correct the bone phenotype in Serpinf1 null mice. *Mol Genet Metab*. 2016;**117**(3):378-382.
80. Belinsky GS, Sreekumar B, Andrejecsk JW, et al. Pigment epithelium-derived factor restoration increases bone mass and improves bone plasticity in a model of osteogenesis imperfecta type VI via Wnt3a blockade. *Faseb J*. 2016;**30**(8):2837-2848.
81. Farber CR, Reich A, Barnes AM, et al. A novel IFITM5 mutation in severe atypical osteogenesis imperfecta type VI impairs osteoblast production of pigment epithelium-derived factor. *J Bone Miner Res*. 2014;**29**(6):1402-1411.
82. Guillén-Navarro E, Ballesta-Martínez MJ, Valencia M, et al. Two mutations in IFITM5 causing distinct forms of osteogenesis imperfecta. *Am J Med Genet A*. 2014;**164A**(5):1136-1142.
83. Hoyer-Kuhn H, Semler O, Garbes L, et al. A nonclassical IFITM5 mutation located in the coding region causes severe osteogenesis imperfecta with prenatal onset. *J Bone Miner Res*. 2014;**29**(6):1387-1391.
84. He Y, Yan JM, Liu YH, Han J, Li DZ. A prenatal case of osteogenesis imperfecta diagnosed with next-generation sequencing. *J Obstet Gynaecol*. 2017;**37**(6):809-810.
85. Liu Y, Asan, Ma D, et al. Gene mutation spectrum and genotype-phenotype correlation in a cohort of Chinese osteogenesis imperfecta patients revealed by targeted next generation sequencing. *Osteoporos Int*. 2017;**28**(10):2985-2995.
86. Chandler N, Best S, Hayward J, et al. Rapid prenatal diagnosis using targeted exome sequencing: a cohort study to assess feasibility and potential impact on prenatal counseling and pregnancy management. *Genet Med*. 2018;**20**(11):1430-1437.
87. Rodriguez Celin M, Moosa S, Fano V. Uncommon IFITM5 mutation associated with severe skeletal deformity in osteogenesis imperfecta. *Ann Hum Genet*. 2018;**82**(6):477-481.
88. Dagdeviren D, Tamimi F, Lee B, Sutton R, Rauch F, Retrouvey JM. Dental and craniofacial characteristics caused by the p.Ser40Leu mutation in IFITM5. *Am J Med Genet A*. 2019;**179**(1):65-70.

89. Guterman-Ram G, Stephan C, Kozloff K, Marini J. New mouse model for atypical type VI osteogenesis imperfecta caused by IFITM5 S40L mutation [abstract]. In: Abstracts of the ECTS Congress 2019. *Calcif Tissue Int*. 2019:104:P321.
90. Berridge MJ. Inositol trisphosphate and calcium signalling mechanisms. *Biochim Biophys Acta*. 2009;**1793**(6):933-940.
91. Meissner G. Monovalent ion and calcium ion fluxes in sarcoplasmic reticulum. *Mol Cell Biochem*. 1983;**55**(1):65-82.
92. Fink RH, Veigel C. Calcium uptake and release modulated by counter-ion conductances in the sarcoplasmic reticulum of skeletal muscle. *Acta Physiol Scand*. 1996;**156**(3):387-396.
93. Yazawa M, Ferrante C, Feng J, et al. TRIC channels are essential for Ca2+ handling in intracellular stores. *Nature*. 2007;**448**(7149):78-82.
94. Gillespie D, Fill M. Intracellular calcium release channels mediate their own countercurrent: the ryanodine receptor case study. *Biophys J*. 2008;**95**(8):3706-3714.
95. Yamazaki D, Komazaki S, Nakanishi H, et al. Essential role of the TRIC-B channel in Ca2+ handling of alveolar epithelial cells and in perinatal lung maturation. *Development*. 2009;**136**(14):2355-2361.
96. Zhou X, Lin P, Yamazaki D, et al. Trimeric intracellular cation channels and sarcoplasmic/endoplasmic reticulum calcium homeostasis. *Circ Res*. 2014;**114**(4):706-716.
97. Venturi E, Matyjaszkiewicz A, Pitt SJ, et al. TRIC-B channels display labile gating: evidence from the TRIC-A knockout mouse model. *Pflugers Arch*. 2013;**465**(8):1135-1148.
98. Shaheen R, Alazami AM, Alshammari MJ, et al. Study of autosomal recessive osteogenesis imperfecta in Arabia reveals a novel locus defined by TMEM38B mutation. *J Med Genet*. 2012;**49**(10):630-635.
99. Volodarsky M, Markus B, Cohen I, et al. A deletion mutation in TMEM38B associated with autosomal recessive osteogenesis imperfecta. *Hum Mutat*. 2013;**34**(4):582-586.
100. Rubinato E, Morgan A, D'Eustacchio A, et al. A novel deletion mutation involving TMEM38B in a patient with autosomal recessive osteogenesis imperfecta. *Gene*. 2014;**545**(2):290-292.
101. Webb EA, Balasubramanian M, Fratzl-Zelman N, et al. Phenotypic spectrum in osteogenesis imperfecta due to mutations in TMEM38B: unraveling a complex cellular defect. *J Clin Endocrinol Metab*. 2017;**102**(6):2019-2028.
102. Lv F, Xu XJ, Wang JY, et al. Two novel mutations in TMEM38B result in rare autosomal recessive osteogenesis imperfecta. *J Hum Genet*. 2016;**61**(6):539-545.
103. Caparros-Martin JA, Aglan MS, Temtamy S, et al. Molecular spectrum and differential diagnosis in patients referred with sporadic or autosomal recessive osteogenesis imperfecta. *Mol Genet Genomic Med*. 2017;**5**(1):28-39.
104. Cabral WA, Ishikawa M, Garten M, et al. Absence of the ER cation channel TMEM38B/TRIC-B disrupts intracellular calcium homeostasis and dysregulates collagen synthesis in recessive osteogenesis imperfecta. *Plos Genet*. 2016;**12**(7):e1006156.
105. Zhao C, Ichimura A, Qian N, et al. Mice lacking the intracellular cation channel TRIC-B have compromised collagen production and impaired bone mineralization. *Sci Signal*. 2016;**9**(428):ra49.
106. Gong Y, Slee RB, Fukai N, et al; Osteoporosis-Pseudoglioma Syndrome Collaborative Group. LDL receptor-related protein 5 (LRP5) affects bone accrual and eye development. *Cell*. 2001;**107**(4):513-523.
107. Boyden LM, Mao J, Belsky J, et al. High bone density due to a mutation in LDL-receptor-related protein 5. *N Engl J Med*. 2002;**346**(20):1513-1521.
108. Ai M, Holmen SL, Van Hul W, Williams BO, Warman ML. Reduced affinity to and inhibition by DKK1 form a common mechanism by which high bone mass-associated missense mutations in LRP5 affect canonical Wnt signaling. *Mol Cell Biol*. 2005;**25**(12):4946-4955.
109. Kato M, Patel MS, Levasseur R, et al. Cbfa1-independent decrease in osteoblast proliferation, osteopenia, and persistent embryonic eye vascularization in mice deficient in Lrp5, a Wnt coreceptor. *J Cell Biol*. 2002;**157**(2):303-314.
110. Babij P, Zhao W, Small C, et al. High bone mass in mice expressing a mutant LRP5 gene. *J Bone Miner Res*. 2003;**18**(6):960-974.
111. Logan CY, Nusse R. The Wnt signaling pathway in development and disease. *Annu Rev Cell Dev Biol*. 2004;**20**:781-810.
112. Fahiminiya S, Majewski J, Mort J, Moffatt P, Glorieux FH, Rauch F. Mutations in WNT1 are a cause of osteogenesis imperfecta. *J Med Genet*. 2013;**50**(5):345-348.
113. Keupp K, Beleggia F, Kayserili H, et al. Mutations in WNT1 cause different forms of bone fragility. *Am J Hum Genet*. 2013;**92**(4):565-574.
114. Pyott SM, Tran TT, Leistritz DF, et al. WNT1 mutations in families affected by moderately severe and progressive recessive osteogenesis imperfecta. *Am J Hum Genet*. 2013;**92**(4):590-597.
115. Laine CM, Joeng KS, Campeau PM, et al. WNT1 mutations in early-onset osteoporosis and osteogenesis imperfecta. *N Engl J Med*. 2013;**368**(19):1809-1816.
116. Stephen J, Girisha KM, Dalal A, et al. Mutations in patients with osteogenesis imperfecta from consanguineous Indian families. *Eur J Med Genet*. 2015;**58**(1):21-27.
117. Umair M, Alhaddad B, Rafique A, et al. Exome sequencing reveals a novel homozygous splice site variant in the WNT1 gene underlying osteogenesis imperfecta type 3. *Pediatr Res*. 2017;**82**(5):753-758.
118. Kausar M, Siddiqi S, Yaqoob M, et al. Correction to: Novel mutation G324C in WNT1 mapped in a large Pakistani family with severe recessively inherited Osteogenesis Imperfecta. *J Biomed Sci*. 2019;**26**(1):31.
119. Lu Y, Ren X, Wang Y, et al. Novel WNT1 mutations in children with osteogenesis imperfecta: Clinical and functional characterization. *Bone*. 2018;**114**:144-149.
120. Kuptanon C, Srichomthong C, Sangsin A, Kovitvanitcha D, Suphapeetiporn K, Shotelersuk V. The most 5' truncating homozygous mutation of WNT1 in siblings with osteogenesis imperfecta with a variable degree of brain anomalies: a case report. *BMC Med Genet*. 2018;**19**(1):117.
121. Kantaputra PN, Sirirungruangsarn Y, Visrutaratna P, et al. WNT1-associated osteogenesis imperfecta with atrophic frontal lobes and arachnoid cysts. *J Hum Genet*. 2019;**64**(4):291-296.
122. Nampoothiri S, Guillemyn B, Elcioglu N, et al. Ptosis as a unique hallmark for autosomal recessive WNT1-associated osteogenesis imperfecta. *Am J Med Genet A*. 2019;**179**(6):908-914.
123. Mäkitie RE, Haanpää M, Valta H, et al. Skeletal characteristics of WNT1 osteoporosis in children and young adults. *J Bone Miner Res*. 2016;**31**(9):1734-1742.

124. Alhamdi S, Lee YC, Chowdhury S, et al. Heterozygous WNT1 variant causing a variable bone phenotype. *Am J Med Genet A*. 2018;**176**(11):2419-2424.
125. McMahon AP, Bradley A. The Wnt-1 (int-1) proto-oncogene is required for development of a large region of the mouse brain. *Cell*. 1990;**62**(6):1073-1085.
126. Aldinger KA, Mendelsohn NJ, Chung BH, et al. Variable brain phenotype primarily affects the brainstem and cerebellum in patients with osteogenesis imperfecta caused by recessive WNT1 mutations. *J Med Genet*. 2016;**53**(6):427-430.
127. Faqeih E, Shaheen R, Alkuraya FS. WNT1 mutation with recessive osteogenesis imperfecta and profound neurological phenotype. *J Med Genet*. 2013;**50**(7):491-492.
128. Joeng KS, Lee YC, Jiang MM, et al. The swaying mouse as a model of osteogenesis imperfecta caused by WNT1 mutations. *Hum Mol Genet*. 2014;**23**(15):4035-4042.
129. Thomas KR, Musci TS, Neumann PE, Capecchi MR. Swaying is a mutant allele of the proto-oncogene Wnt-1. *Cell*. 1991;**67**(5):969-976.
130. Joeng KS, Lee YC, Lim J, et al. Osteocyte-specific WNT1 regulates osteoblast function during bone homeostasis. *J Clin Invest*. 2017;**127**(7):2678-2688.
131. Wang F, Tarkkonen K, Nieminen-Pihala V, et al. Mesenchymal cell-derived juxtacrine Wnt1 signaling regulates osteoblast activity and osteoclast differentiation. *J Bone Miner Res*. 2019;**34**(6):1129-1142.
132. Moosa S, Yamamoto GL, Garbes L, et al. Autosomal-recessive mutations in MESD cause osteogenesis imperfecta. *Am J Hum Genet*. 2019;**105**(4):836-843.
133. Stürznickel J, Jähn-Rickert K, Zustin J, et al. Compound heterozygous frameshift mutations in MESD cause a lethal syndrome suggestive of osteogenesis imperfecta type XX. *J Bone Miner Res*. Published online February 2021. doi:10.1002/jbmr.4277
134. Holdener BC, Faust C, Rosenthal NS, Magnuson T. msd is required for mesoderm induction in mice. *Development*. 1994;**120**(5):1335-1346.
135. Hsieh JC, Lee L, Zhang L, et al. Mesd encodes an LRP5/6 chaperone essential for specification of mouse embryonic polarity. *Cell*. 2003;**112**(3):355-367.
136. Honma Y, Kanazawa K, Mori T, et al. Identification of a novel gene, OASIS, which encodes for a putative CREB/ATF family transcription factor in the long-term cultured astrocytes and gliotic tissue. *Brain Res Mol Brain Res*. 1999;**69**(1):93-103.
137. Omori Y, Imai J, Suzuki Y, Watanabe S, Tanigami A, Sugano S. OASIS is a transcriptional activator of CREB/ATF family with a transmembrane domain. *Biochem Biophys Res Commun*. 2002;**293**(1):470-477.
138. Kondo S, Murakami T, Tatsumi K, et al. OASIS, a CREB/ATF-family member, modulates UPR signalling in astrocytes. *Nat Cell Biol*. 2005;**7**(2):186-194.
139. Murakami T, Kondo S, Ogata M, et al. Cleavage of the membrane-bound transcription factor OASIS in response to endoplasmic reticulum stress. *J Neurochem*. 2006;**96**(4):1090-1100.
140. Murakami T, Hino S, Nishimura R, Yoneda T, Wanaka A, Imaizumi K. Distinct mechanisms are responsible for osteopenia and growth retardation in OASIS-deficient mice. *Bone*. 2011;**48**(3):514-523.
141. Symoens S, Malfait F, D'hondt S, et al. Deficiency for the ER-stress transducer OASIS causes severe recessive osteogenesis imperfecta in humans. *Orphanet J Rare Dis*. 2013;**8**:154.
142. Keller RB, Tran TT, Pyott SM, et al. Monoallelic and biallelic CREB3L1 variant causes mild and severe osteogenesis imperfecta, respectively. *Genet Med*. 2018;**20**(4):411-419.
143. Guillemyn B, Kayserili H, Demuynck L, et al. A homozygous pathogenic missense variant broadens the phenotypic and mutational spectrum of CREB3L1-related osteogenesis imperfecta. *Hum Mol Genet*. 2019;**28**(11):1801-1809.
144. Lindahl K, Åström E, Dragomir A, et al. Homozygosity for CREB3L1 premature stop codon in first case of recessive osteogenesis imperfecta associated with OASIS-deficiency to survive infancy. *Bone*. 2018;**114**:268-277.
145. Cayami FK, Maugeri A, Treurniet S, et al. The first family with adult osteogenesis imperfecta caused by a novel homozygous mutation in CREB3L1. *Mol Genet Genomic Med*. 2019;**7**(8):e823.
146. Brown MS, Ye J, Rawson RB, Goldstein JL. Regulated intramembrane proteolysis: a control mechanism conserved from bacteria to humans. *Cell*. 2000;**100**(4):391-398.
147. Rawson RB. Regulated intramembrane proteolysis: from the endoplasmic reticulum to the nucleus. *Essays Biochem*. 2002;**38**:155-168.
148. Ye J, Rawson RB, Komuro R, et al. ER stress induces cleavage of membrane-bound ATF6 by the same proteases that process SREBPs. *Mol Cell*. 2000;**6**(6):1355-1364.
149. Wang X, Sato R, Brown MS, Hua X, Goldstein JL. SREBP-1, a membrane-bound transcription factor released by sterol-regulated proteolysis. *Cell*. 1994;**77**(1):53-62.
150. Lindert U, Cabral WA, Ausavarat S, et al. MBTPS2 mutations cause defective regulated intramembrane proteolysis in X-linked osteogenesis imperfecta. *Nat Commun*. 2016;**7**:11920.
151. Oeffner F, Fischer G, Happle R, et al. IFAP syndrome is caused by deficiency in MBTPS2, an intramembrane zinc metalloprotease essential for cholesterol homeostasis and ER stress response. *Am J Hum Genet*. 2009;**84**(4):459-467.
152. Naiki M, Mizuno S, Yamada K, et al. MBTPS2 mutation causes BRESEK/BRESHECK syndrome. *Am J Med Genet A*. 2012;**158A**(1):97-102.
153. Aten E, Brasz LC, Bornholdt D, et al. Keratosis Follicularis Spinulosa Decalvans is caused by mutations in MBTPS2. *Hum Mutat*. 2010;**31**(10):1125-1133.
154. Kondo Y, Fu J, Wang H, et al. Site-1 protease deficiency causes human skeletal dysplasia due to defective inter-organelle protein trafficking. *JCI Insight*. 2018;**3**(14):e121596.
155. Patra D, Xing X, Davies S, et al. Site-1 protease is essential for endochondral bone formation in mice. *J Cell Biol*. 2007;**179**(4):687-700.
156. Patra D, DeLassus E, Mueller J, Abou-Ezzi G, Sandell LJ. Site-1 protease regulates skeletal stem cell population and osteogenic differentiation in mice. *Biol Open*. 2018;**7**(2):bio032094.
157. Dubail J, Brunelle P, Baujat G, et al. Homozygous loss-of-function mutations in CCDC134 are responsible for a severe form of osteogenesis imperfecta. *J Bone Miner Res*. 2020;**35**(8):1470-1480.

158. Huang J, Shi T, Ma T, et al. CCDC134, a novel secretory protein, inhibits activation of ERK and JNK, but not p38 MAPK. *Cell Mol Life Sci*. 2008;**65**(2):338-349.
159. Yu B, Zhang T, Xia P, Gong X, Qiu X, Huang J. CCDC134 serves a crucial role in embryonic development. *Int J Mol Med*. 2018;**41**(1):381-390.
160. de la Croix Ndong J, Stevens DM, Vignaux G, et al. Combined MEK inhibition and BMP2 treatment promotes osteoblast differentiation and bone healing in Nf1Osx$^{-/-}$ mice. *J Bone Miner Res*. 2015;**30**(1):55-63.
161. Kang H, Jha S, Deng Z, et al. Somatic activating mutations in MAP2K1 cause melorheostosis. *Nat Commun*. 2018;**9**(1):1-12.
162. van Dijk FS, Semler O, Etich J, et al. Interaction between KDELR2 and HSP47 as a key determinant in osteogenesis imperfecta caused by bi-allelic variants in KDELR2. *Am J Hum Genet*. 2020;**107**(5):989-999.
163. Capitani M, Sallese M. The KDEL receptor: new functions for an old protein. *FEBS Lett*. 2009;**583**(23):3863-3871.
164. Bräuer P, Parker JL, Gerondopoulos A, et al. Structural basis for pH-dependent retrieval of ER proteins from the Golgi by the KDEL receptor. *Science*. 2019;**363**(6431):1103-1107.
165. Pobre KFR, Poet GJ, Hendershot LM. The endoplasmic reticulum (ER) chaperone BiP is a master regulator of ER functions: getting by with a little help from ERdj friends. *J Biol Chem*. 2019;**294**(6):2098-2108.
166. Roschger P, Fratzl-Zelman N, Misof BM, Glorieux FH, Klaushofer K, Rauch F. Evidence that abnormal high bone mineralization in growing children with osteogenesis imperfecta is not associated with specific collagen mutations. *Calcif Tissue Int*. 2008;**82**(4):263-270.
167. Fratzl-Zelman N, Morello R, Lee B, et al. CRTAP deficiency leads to abnormally high bone matrix mineralization in a murine model and in children with osteogenesis imperfecta type VII. *Bone*. 2010;**46**(3):820-826.
168. Fratzl-Zelman N, Schmidt I, Roschger P, et al. Unique micro- and nano-scale mineralization pattern of human osteogenesis imperfecta type VI bone. *Bone*. 2015;**73**:233-241.
169. Sweeney SM, Orgel JP, Fertala A, et al. Candidate cell and matrix interaction domains on the collagen fibril, the predominant protein of vertebrates. *J Biol Chem*. 2008;**283**(30):21187-21197.
170. Uveges TE, Collin-Osdoby P, Cabral WA, et al. Cellular mechanism of decreased bone in Brtl mouse model of OI: imbalance of decreased osteoblast function and increased osteoclasts and their precursors. *J Bone Miner Res*. 2008;**23**(12):1983-1994.
171. Rauch F, Travers R, Parfitt AM, Glorieux FH. Static and dynamic bone histomorphometry in children with osteogenesis imperfecta. *Bone*. 2000;**26**(6):581-589.
172. Saban J, Zussman MA, Havey R, Patwardhan AG, Schneider GB, King D. Heterozygous oim mice exhibit a mild form of osteogenesis imperfecta. *Bone*. 1996;**19**(6):575-579.
173. Cabral WA, Perdivara I, Weis M, et al. Abnormal type I collagen post-translational modification and crosslinking in a cyclophilin B KO mouse model of recessive osteogenesis imperfecta. *PLoS Genet*. 2014;**10**(6):e1004465.
174. Eyre DR, Weis MA, Wu JJ. Advances in collagen cross-link analysis. *Methods*. 2008;**45**(1):65-74.
175. Carriero A, Zimmermann EA, Paluszny A, et al. How tough is brittle bone? Investigating osteogenesis imperfecta in mouse bone. *J Bone Miner Res*. 2014;**29**(6):1392-1401.
176. Boyde A, Travers R, Glorieux FH, Jones SJ. The mineralization density of iliac crest bone from children with osteogenesis imperfecta. *Calcif Tissue Int*. 1999;**64**(3):185-190.
177. Roschger P, Paschalis EP, Fratzl P, Klaushofer K. Bone mineralization density distribution in health and disease. *Bone*. 2008;**42**(3):456-466.
178. Pabisch S, Wagermaier W, Zander T, Li C, Fratzl P. Imaging the nanostructure of bone and dentin through small- and wide-angle X-ray scattering. *Methods Enzymol*. 2013;**532**:391-413.
179. Fratzl P, Paris O, Klaushofer K, Landis WJ. Bone mineralization in an osteogenesis imperfecta mouse model studied by small-angle x-ray scattering. *J Clin Invest*. 1996;**97**(2):396-402.
180. Fratzl-Zelman N, Schmidt I, Roschger P, et al. Mineral particle size in children with osteogenesis imperfecta type I is not increased independently of specific collagen mutations. *Bone*. 2014;**60**:122-128.
181. Fratzl-Zelman N, Barnes AM, Weis M, et al. Non-lethal Type VIII osteogenesis imperfecta has elevated bone matrix mineralization. *J Clin Endocrinol Metab*. 2016;**101**(9):3516-3525.
182. Hoyer-Kuhn H, Semler O, Schoenau E, Roschger P, Klaushofer K, Rauch F. Hyperosteoidosis and hypermineralization in the same bone: bone tissue analyses in a boy with a homozygous BMP1 mutation. *Calcif Tissue Int*. 2013;**93**(6):565-570.
183. Barnes AM, Chang W, Morello R, et al. Deficiency of cartilage-associated protein in recessive lethal osteogenesis imperfecta. *N Engl J Med*. 2006;**355**(26):2757-2764.
184. Barnes AM, Carter EM, Cabral WA, et al. Lack of cyclophilin B in osteogenesis imperfecta with normal collagen folding. *N Engl J Med*. 2010;**362**(6):521-528.
185. Homan EP, Lietman C, Grafe I, et al. Differential effects of collagen prolyl 3-hydroxylation on skeletal tissues. *PLoS Genet*. 2014;**10**(1):e1004121.
186. Palomo T, Al-Jallad H, Moffatt P, et al. Skeletal characteristics associated with homozygous and heterozygous WNT1 mutations. *Bone*. 2014;**67**:63-70.
187. Engelbert RH, Uiterwaal CS, Gerver WJ, van der Net JJ, Pruijs HE, Helders PJ. Osteogenesis imperfecta in childhood: impairment and disability: a prospective study with 4-year follow-up. *Arch Phys Med Rehabil*. 2004;**85**(5):772-778.
188. Sousa T, Bompadre V, White KK. Musculoskeletal functional outcomes in children with osteogenesis imperfecta: associations with disease severity and pamidronate therapy. *J Pediatr Orthop*. 2014;**34**(1):118-122.
189. Esposito P, Plotkin H. Surgical treatment of osteogenesis imperfecta: current concepts. *Curr Opin Pediatr*. 2008;**20**(1):52-57.
190. Azzam KA, Rush ET, Burke BR, Nabower AM, Esposito PW. Mid-term results of femoral and tibial osteotomies and fassier-duval nailing in children with osteogenesis imperfecta. *J Pediatr Orthop*. 2018;**38**(6):331-336.
191. Yilmaz G, Hwang S, Oto M, et al. Surgical treatment of scoliosis in osteogenesis imperfecta with cement-augmented pedicle screw instrumentation. *J Spinal Disord Tech*. 2014;**27**(3):174-180.

192. Castelein RM, Hasler C, Helenius I, Ovadia D, Yazici M; EPOS Spine Study Group. Complex spine deformities in young patients with severe osteogenesis imperfecta: current concepts review. *J Child Orthop*. 2019;**13**(1):22-32.
193. Papagelopoulos PJ, Morrey BF. Hip and knee replacement in osteogenesis imperfecta. *J Bone Joint Surg Am*. 1993;**75**(4):572-580.
194. Retrouvey JM, Taqi D, Tamimi F, et al; Members of the BBD Consortium. Oro-dental and cranio-facial characteristics of osteogenesis imperfecta type V. *Eur J Med Genet*. 2019;**62**(12):103606.
195. Folkestad L, Hald JD, Canudas-Romo V, et al. Mortality and causes of death in patients with osteogenesis imperfecta: A register-based nationwide cohort study. *J Bone Miner Res*. 2016;**31**(*12*):2159-2166.
196. Widmann RF, Bitan FD, Laplaza FJ, Burke SW, DiMaio MF, Schneider R. Spinal deformity, pulmonary compromise, and quality of life in osteogenesis imperfecta. *Spine (Phila Pa 1976)*. 1999;**24**(16):1673-1678.
197. Baldridge D, Lennington J, Weis M, et al. Generalized connective tissue disease in Crtap$^{-/-}$ mouse. *PLoS One*. 2010;**5**(5):e10560.
198. Radunovic Z, Wekre LL, Diep LM, Steine K. Cardiovascular abnormalities in adults with osteogenesis imperfecta. *Am Heart J*. 2011;**161**(3):523-529.
199. Kuurila K, Grénman R, Johansson R, Kaitila I. Hearing loss in children with osteogenesis imperfecta. *Eur J Pediatr*. 2000;**159**(7):515-519.
200. Martens S, Dhooge IJM, Swinnen FKR. Longitudinal analysis of the audiological phenotype in osteogenesis imperfecta: a follow-up study. *J Laryngol Otol*. 2018;**132**(8):703-710.
201. Pillion JP, Vernick D, Shapiro J. Hearing loss in osteogenesis imperfecta: characteristics and treatment considerations. *Genet Res Int*. 2011;**2011**:983942.
202. Charnas LR, Marini JC. Communicating hydrocephalus, basilar invagination, and other neurologic features in osteogenesis imperfecta. *Neurology*. 1993;**43**(12):2603-2608.
203. Menezes AH. Specific entities affecting the craniocervical region. *Child's Nerv Syst*. 2008;*24*(10):1169-1172.
204. Arponen H, Vuorimies I, Haukka J, Valta H, Waltimo-Sirén J, Mäkitie O. Cranial base pathology in pediatric osteogenesis imperfecta patients treated with bisphosphonates. *J Neurosurg Pediatr*. 2015;**15**(3):313-320.
205. Marini JC, Forlino A, Bächinger HP, et al. Osteogenesis imperfecta. *Nat Rev Dis Primers*. 2017;**3**(1):1-19.
206. Bains JS, Carter EM, Citron KP, et al; Members of the BBD Consortium. A multicenter observational cohort study to evaluate the effects of bisphosphonate exposure on bone mineral density and other health outcomes in osteogenesis imperfecta. *JBMR Plus*. 2019;**3**(5):e10118.
207. Letocha AD, Cintas HL, Troendle JF, et al. Controlled trial of pamidronate in children with types III and IV osteogenesis imperfecta confirms vertebral gains but not short-term functional improvement. *J Bone Miner Res*. 2005;**20**(6):977-986.
208. Bishop N, Adami S, Ahmed SF, et al. Risedronate in children with osteogenesis imperfecta: a randomised, double-blind, placebo-controlled trial. *Lancet*. 2013;**382**(9902):1424-1432.
209. Dwan K, Phillipi CA, Steiner RD, Basel D. Bisphosphonate therapy for osteogenesis imperfecta. *Cochrane Database Syst Rev*. 2014;7;CD005088.
210. Dwan K, Phillipi CA, Steiner RD, Basel D. Bisphosphonate therapy for osteogenesis imperfecta. *Cochrane Database Syst Rev*. 2016;**10**(10):CD005088.
211. Hald JD, Evangelou E, Langdahl BL, Ralston SH. Bisphosphonates for the prevention of fractures in osteogenesis imperfecta: meta-analysis of placebo-controlled trials. *J Bone Miner Res*. 2015;**30**(5):929-933.
212. Sato A, Ouellet J, Muneta T, Glorieux FH, Rauch F. Scoliosis in osteogenesis imperfecta caused by COL1A1/COL1A2 mutations–genotype-phenotype correlations and effect of bisphosphonate treatment. *Bone*. 2016;**86**:53-57.
213. Rauch F, Cornibert S, Cheung M, Glorieux FH. Long-bone changes after pamidronate discontinuation in children and adolescents with osteogenesis imperfecta. *Bone*. 2007;**40**(4):821-827.
214. Sinder BP, Eddy MM, Ominsky MS, Caird MS, Marini JC, Kozloff KM. Sclerostin antibody improves skeletal parameters in a Brtl/+ mouse model of osteogenesis imperfecta. *J Bone Miner Res*. 2013;**28**(1):73-80.
215. Sinder BP, White LE, Salemi JD, et al. Adult Brtl/+ mouse model of osteogenesis imperfecta demonstrates anabolic response to sclerostin antibody treatment with increased bone mass and strength. *Osteoporos Int*. 2014;**25**(8):2097-2107.
216. Jacobsen CM, Barber LA, Ayturk UM, et al. Targeting the LRP5 pathway improves bone properties in a mouse model of osteogenesis imperfecta. *J Bone Miner Res*. 2014;**29**(10):2297-2306.
217. Grafe I, Alexander S, Yang T, et al. Sclerostin antibody treatment improves the bone phenotype of Crtap$^{-/-}$ mice, a model of recessive osteogenesis imperfecta. *J Bone Miner Res*. 2016;**31**(5):1030-1040.
218. Grafe I, Yang T, Alexander S, et al. Excessive transforming growth factor-β signaling is a common mechanism in osteogenesis imperfecta. *Nat Med*. 2014;**20**(6):670-675.
219. Perosky JE, Khoury BM, Jenks TN, et al. Single dose of bisphosphonate preserves gains in bone mass following cessation of sclerostin antibody in Brtl/+ osteogenesis imperfecta model. *Bone*. 2016;**93**:79-85.
220. Little DG, Peacock L, Mikulec K, et al. Combination sclerostin antibody and zoledronic acid treatment outperforms either treatment alone in a mouse model of osteogenesis imperfecta. *Bone*. 2017;**101**:96-103.
221. Besio R, Forlino A. New frontiers for dominant osteogenesis imperfecta treatment: gene/cellular therapy approaches. *Adv Regen Biol*. 2015;**2**(*1*):27964.
222. Guillot PV, Abass O, Bassett JH, et al. Intrauterine transplantation of human fetal mesenchymal stem cells from first-trimester blood repairs bone and reduces fractures in osteogenesis imperfecta mice. *Blood*. 2008;**111**(3):1717-1725.
223. Panaroni C, Gioia R, Lupi A, et al. In utero transplantation of adult bone marrow decreases perinatal lethality and rescues the bone phenotype in the knockin murine model for classical, dominant osteogenesis imperfecta. *Blood*. 2009;**114**(2):459-468.
224. Sinder BP, Novak S, Wee NKY, et al. Engraftment of skeletal progenitor cells by bone-directed transplantation improves osteogenesis imperfecta murine bone phenotype. *Stem Cells*. 2020;**38**(4):530-541.